Supporting Information

Exploring Halogen···Halogen Interactions in Supramolecular Self-Assembly of BODIPY Networks

Burcu Topaloğlu Aksoy,[a] Burcu Dedeoglu,[a] Yunus Zorlu,[a] Mehmet Menaf Ayhan*[a] Bünyemin Çoşut,*[a]

[a] Department of Chemistry, Faculty of Science, Gebze Technical University, Gebze, Kocaeli, Turkiye

Correspondence:

menafayhan@gtu.edu.tr, bcosut@gtu.edu.tr

TABLE OF CONTENTS

1. EXPERIMENTAL SECTION

1.1. Materials and Characterization Equipment

Commercially available chemicals were purchased from Aldrich and all solvents for the synthesis, purification, and characterization were acquired from Merck. Reaction progresses were monitored by thin layer chromatography using Merck TLC Silica gel 60 F_{254}. Silica gel column chromatography was performed using Merck Silica gel 60 (particle size: 0.040-0.063 mm, 230-400 mesh ASTM). Mass analyses were recorded on a Bruker MS MALDI TOF spectrometer (Bremen, Germany) using 2,5-dihydroxybenzoic acid as a matrix. ^{1}H and ^{13}C NMR spectra were lined out for all compounds in $CDCl_3$ on a Varian INOVA 500 MHz spectrometer (West Sussex, UK) using TMS as an internal reference for ^{1}H and ^{13}C measurements. Electronic absorption spectra in the UV-Vis region were measured with a Shimadzu 2101 UV-Vis spectrophotometer (Tokyo, Japan).

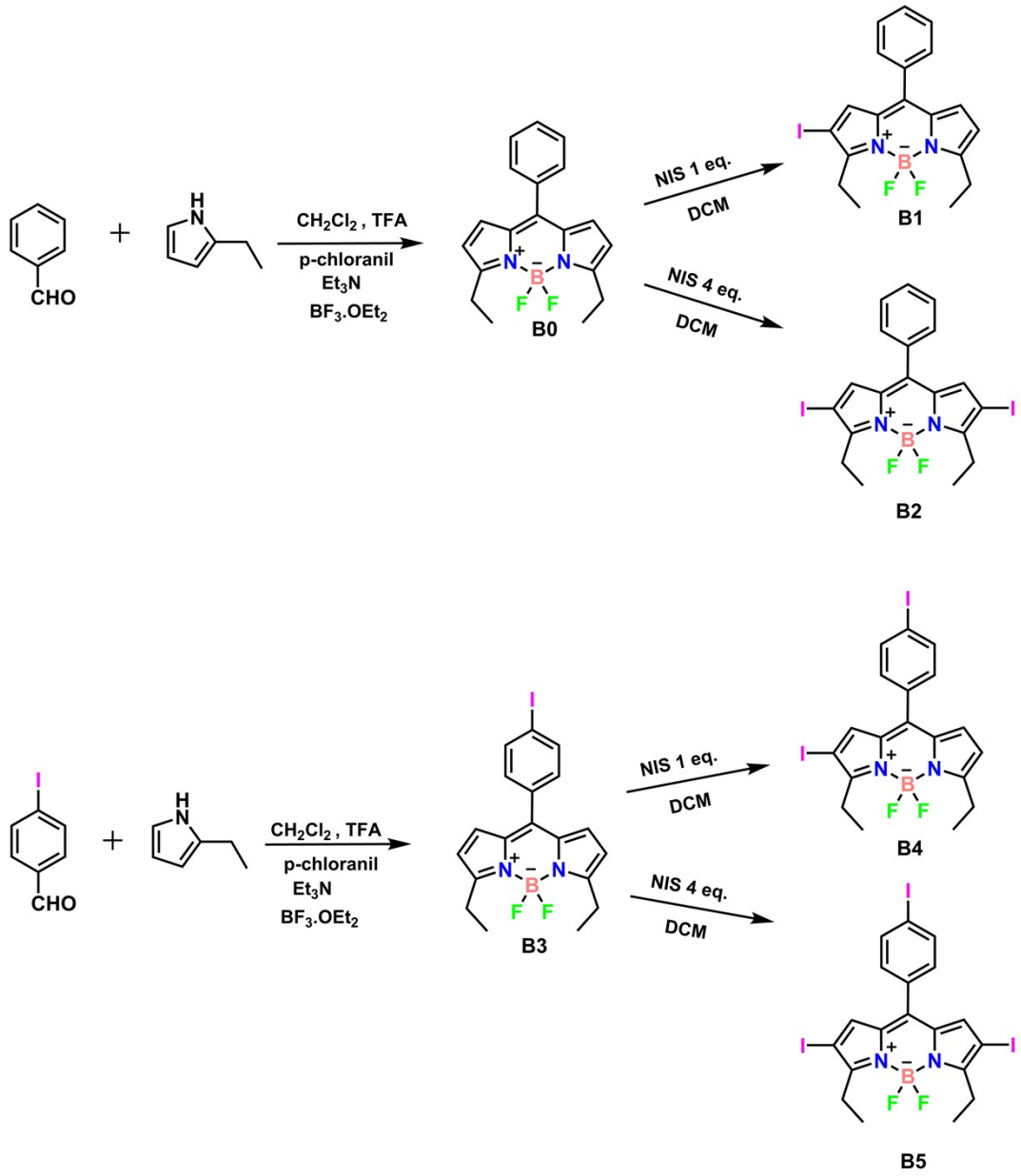

Scheme S1. Chemical structure and synthetic pathway of BODIPY Derivatives

1.1. Synthesis and Characterizations

The compounds **B0** and **B3** were synthesized and purified according to literature.[1] Compound **B1**, **B2**, **B4,** and **B5** were synthesized and purified according to modified literature.[2] The treatment of benzaldehyde with 2,4-diethylpyrrole in the presence of trifluoroacetic acid in dichloromethane afforded the dipyrromethane which was subsequently oxidized into corresponding dipyrromethene, prior to its complexation in BF_3-OEt_2, producing the meso-

benzaldehyde linked BODIPY (**B0**). Compound **B0** was reacted with NIS (N-iodosuccinimide) at a 1:1 and 1:4 molar ratio in CH_2Cl_2 at room temperature, and mono-halogenated BODIPY (**B1**) and dihalogenated BODIPY (**B2**) were obtained, respectively (Scheme S1). 4-Iodo Benzaldehyde was treated with 2,4-diethylpyrrole to yield compound **B3** by using the classic BODIPY synthesis method. 2,6 Positions of compound **B3** were decorated with iodine atoms (compound **B4** and **B5**). The BODIPY derivatives were purified by column chromatography and the structures of BODIPY compounds were supported by ^{1}H NMR, ^{13}C NMR and mass spectrometry.

1.1.1. Synthesis of Compound B0

CH_2Cl_2 (300 ml) was placed in a 1 L of round bottom reaction flask and it was purged with argon gas for 15 min. Benzaldehyde (1 g, 9.43 mmol) and 2-ethylpyrrole (1.95 mL, 18.8 mmol) were added to the medium, respectively. The color of the solution turned to red after the addition of 2 drops of trifluoroacetic acid. The reaction mixture was stirred at room temperature for 12 h. After 12 h, p-chloranil (2.3 g, 9.43 mmol) was added to the reaction medium and the mixture was stirred at room temperature for a further 30 min. Then, triethyl amine (6 mL) and boron trifluoride diethyl etherate ($BF_3.OEt_2$) (6 mL) were added, sequentially. The reaction mixture was stirred at room temperature for further 3 hours. Then, it was extracted with CH_2Cl_2 and water. Organic layer was dried with Na_2SO_4 and evaporated under reduced pressure. The crude product was purified by silica gel column chromatography using CH_2Cl_2 - n-hexane (3:2) as mobile phase. Fraction containing compound **B0** was collected then the solvent was removed under reduced pressure (0.34 mmol, 110 mg, 3.6%). MALDI TOF (m/z) calc. 324.16, found: 324.034 $[M^+]$ ^{1}H NMR (500 MHz, $CDCl_3$) δ_H 7.53 (m, 3H), (Ar-CH), 7.51 (m, 2H), (Ar-CH), 6.75 (d, J = 5 Hz, 2H), (Ar-CH), 6.35 (d, J = 45 Hz, 2H), (Ar-CH), 3.11 (q, J= 7.8 Hz, 4H), (CH_2), 1.36 (t, J= 7.8 Hz, 3H), (CH_3) ppm.^{13}C NMR (126 MHz, $CDCl_3$) δ_C 163.56, 142.88, 134.25, 130.48, 130.37, 129.87, 128.15, 11.26, 117.23, 22.05, 12.79 ppm.

1.1.2. Synthesis of Compound B1

Compound **1** (70 mg, 0.22 mmol) was dissolved with 20 mL of CH_2Cl_2. N-iodo-succinimide (NIS) (72 mg, 0.23 mmol) was added to the previous reaction mixture and it was stirred for 30 minutes. According to thin layer chromatography tests, it was stirred additional 3 hours and then solvent of the reaction was evaporated under reduced pressure. The crude product was purified by silica gel column chromatography using n-hexane–CH_2Cl_2 (2:1) as mobile phase. Fraction containing compound **B1** was collected then the solvent was removed under reduced pressure (0.12 mmol, 55 mg, 54%). MALDI TOF (m/z) calc. 450.06, found: 450.106 [M^+] ^{1}H NMR (500 MHz, $CDCl_3$) δ_H 7.54 (m, 1H), (Ar-CH), 7.5 (m, 2H), (Ar-CH), 7.4 (broad, 2H), (Ar-CH), 6.87 (s, 1H), (Ar-CH), 6.82 (d, J= 4.3 Hz, 1H), (Ar-CH), 6.4 (d, J= 4.3 Hz, 1H), (Ar-CH), 3.1 (q, J= 7.5 Hz, 2H) (CH_2), 3.03 (q, J= 7.5 Hz, 2H) (CH_2), 1.37 (t, J= 6 Hz, 3H) (CH_3), 1.34 (t, J= 6 Hz, 3H) (CH_3), ppm.^{13}C NMR (126 MHz, $CDCl_3$) δ_C 164.76, 160.25, 141.16, 134.58, 133.77, 133.48, 132.72, 131.09, 129.28, 129.16, 127.30, 117.62, 117.58, 21.70, 21.22, 12.44, 11.60 ppm.

1.1.3. Synthesis of Compound B2

Compound **1** (70 mg, 0.22 mmol) was dissolved with 20 mL of CH_2Cl_2. N-iodo-succinimide (NIS) (277 mg, 0.88 mmol) was added to the previous reaction mixture and it was stirred for 30 minutes. According to thin layer chromatography tests, it was stirred additional 3 hours and then solvent of the reaction was evaporated under reduced pressure. The crude product was purified by silica gel column chromatography using n-hexane–CH_2Cl_2 (2:1) as mobile phase. Fraction containing compound **B2** was collected then the solvent was removed under reduced pressure (0.026 mmol, 15 mg, 12%). MALDI TOF (m/z) calc. 575.95, found: 575.158 [M^+] ^{1}H NMR (500 MHz, $CDCl_3$) δ_H 7.56 (m, 1H), (Ar-CH), 7.51 (m, 2H), (Ar-CH), 7.4 (m, 2H), (Ar-CH), 6.96 (s, 2H), (Ar-CH), 3.05 (m, 4H) (CH_2), 1.35 (m, 6H) (CH_3), ppm.^{13}C NMR (126 MHz,

$CDCl_3$) δ_C 164.03, 140.08, 137.95, 134.92, 132.89, 131.84, 97.24, 68.13, 53.56, 32.08, 29.85, 29.51, 25.77, 23.08, 22.85, 14.27, 13.42 ppm.

1.1.4. Synthesis of Compound B3

CH_2Cl_2 (300 ml) was placed in a 1 L of round bottom reaction flask and it was purged with argon gas for 15 min. 4-iodo benzaldehyde (1 g, 4.3 mmol) and 2-ethylpyrrole (0.88 mL, 8.6 mmol) were added to the medium, respectively. The color of the solution turned to red after the addition of 3 drops of trifluoroacetic acid. The reaction mixture was stirred at room temperature for 12 h. After 12 h, p-chloranil (1 g, 4.3 mmol) was added to the reaction medium and the mixture was stirred at room temperature for a further 30 min. Then, triethyl amine (5 mL) and boron trifluoride diethyl etherate ($BF_3.OEt_2$) (6 mL) were added, sequentially. The reaction mixture was stirred at room temperature for further 3 hours. Then, it was extracted with CH_2Cl_2 and water. Organic layer was dried with Na_2SO_4 and evaporated under reduced pressure. The crude product was purified by silica gel column chromatography using n-hexane–CH_2Cl_2 (1:1) as mobile phase. Fraction containing compound **B3** was collected then the solvent was removed under reduced pressure (0.8 mmol, 363 mg, 19 %). MALDI TOF (m/z) calc. 450.06, found: 450.064 [M^+] ^{1}H NMR (500 MHz, $CDCl_3$) δ_H 7.84 (d, J = 8.6 Hz, 2H), (Ar-CH), 7.26 (d, J = 8.5 Hz, 2H), (Ar-CH), 6.71 (d, J = 4.9 Hz, 2H), (Ar-CH), 6.36 (d, J = 4.9 Hz, 2H), (Ar-CH), 3.10 (q, 4H), (CH_2), 1.36 (t, J= 7.8 Hz, 3H), (CH_3) ppm.^{13}C NMR (126 MHz, $CDCl_3$) δ_C 164.03, 141.34, 137.45, 133.91, 133.70, 131.90, 130.17, 117.53, 96.29, 22.07, 12.76 ppm.

1.1.5. Synthesis of Compound B4

Compound **B3** (100 mg, 0.22 mmol) was dissolved with 50 mL of CH_2Cl_2 and the mixture was purged with Ar for 10 min. N-iodo-succinimide (54 mg, 0.24 mmol) (NIS) was dissolved in 10 ml of CH_2Cl_2 and added dropwise to the previous reaction medium at 10-15°C. Reaction mixture was stirred for 1 hour under argon atmosphere. Then, the resulting mixture was extracted with

CH_2Cl_2 and water. The organic layer was dried with Na_2SO_4 and evaporated under reduced pressure. The crude product was purified by silica gel column chromatography using n-hexane–CH_2Cl_2 (2:1) as mobile phase. Fraction containing compound **B4** was collected then the solvent was removed under reduced pressure (0.069 mmol, 40 mg, 31.5 %). MALDI TOF (m/z) calc. 575.95, found: 575.288 [M^+] ^{1}H NMR (500 MHz, $CDCl_3$) δ_H 7.78 (d, J = 6.5 Hz, 2H), (Ar-CH), 7.15 (d, J = 6.5 Hz, 2H), (Ar-CH), 6.77 (s, 1H), (Ar-CH), 6.72 (d, J = 4.3 Hz, 1H), (Ar-CH), 6.36 (d, J = 4.3 Hz, 1H), (Ar-CH), 3.03 (q, J= 7.6 Hz, 2H), (CH_2), 2.96 (q, J= 7.5 Hz, 2H), (CH_2), 1.29 (m, 6H), (CH_3) ppm.^{13}C NMR (126 MHz, $CDCl_3$) δ_C 165.20, 160.74, 139.60, 136.60, 134.31, 133.43, 133.13, 132.15, 130.76, 130.72, 117.91, 117.88, 95.68, 21.72, 21.25, 12.41, 11.57 ppm.

1.1.6. Synthesis of Compound B5

Compound **B3** (200 mg, 0.44 mmol) was dissolved with 50 mL of CH_2Cl_2 and the mixture was purged with Ar for 10 min. N-iodo-succinimide (396 mg, 1.76 mmol) (NIS) was dissolved in 10 ml of CH_2Cl_2 and added dropwise to the previous reaction medium at 10-15°C. Reaction mixture was stirred for 1 hour under argon atmosphere. Then, the resulting mixture was extracted with CH_2Cl_2 and water. The organic layer was dried with Na_2SO_4 and evaporated under reduced pressure. The crude product was purified by silica gel column chromatography using n-hexane–CH_2Cl_2 (2:1) as mobile phase. Fraction containing compound **B5** was collected then the solvent was removed under reduced pressure (0.028 mmol, 20 mg, 6.5%). MALDI TOF (m/z) calc. 701.85, found: 701.018 [M^+] 7.87 (d, J = 6.6 Hz, 2H), (Ar-CH), 7.22 (d, J = 6.5 Hz, 2H), (Ar-CH), 6.93 (s, 2H), (Ar-CH), 3.04 (q, 4H), (CH_2), 1.34 (m, 6H), (CH_3) ppm.^{13}C NMR (126 MHz, $CDCl_3$) δ_C 163.56, 141.66, 137.40, 135.75, 135.16, 133.48, 132.25, 130.65, 130.45, 130.40, 130.33, 128.64, 128.47, 118.78, 68.13, 53.57, 32.09, 29.86, 29.52, 23.06, 22.86, 14.28, 13.61, 13.46, 12.78 ppm.

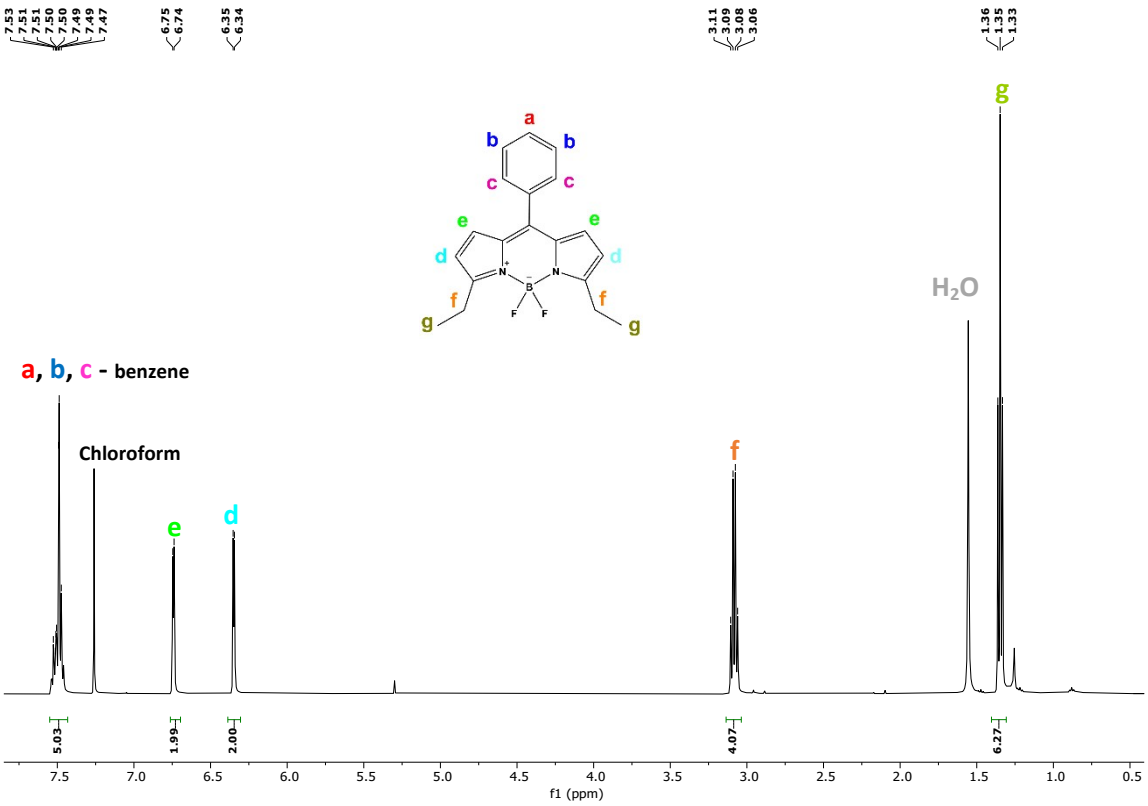

Figure S1: ^{1}H NMR Spectrum of the Compound **B0**

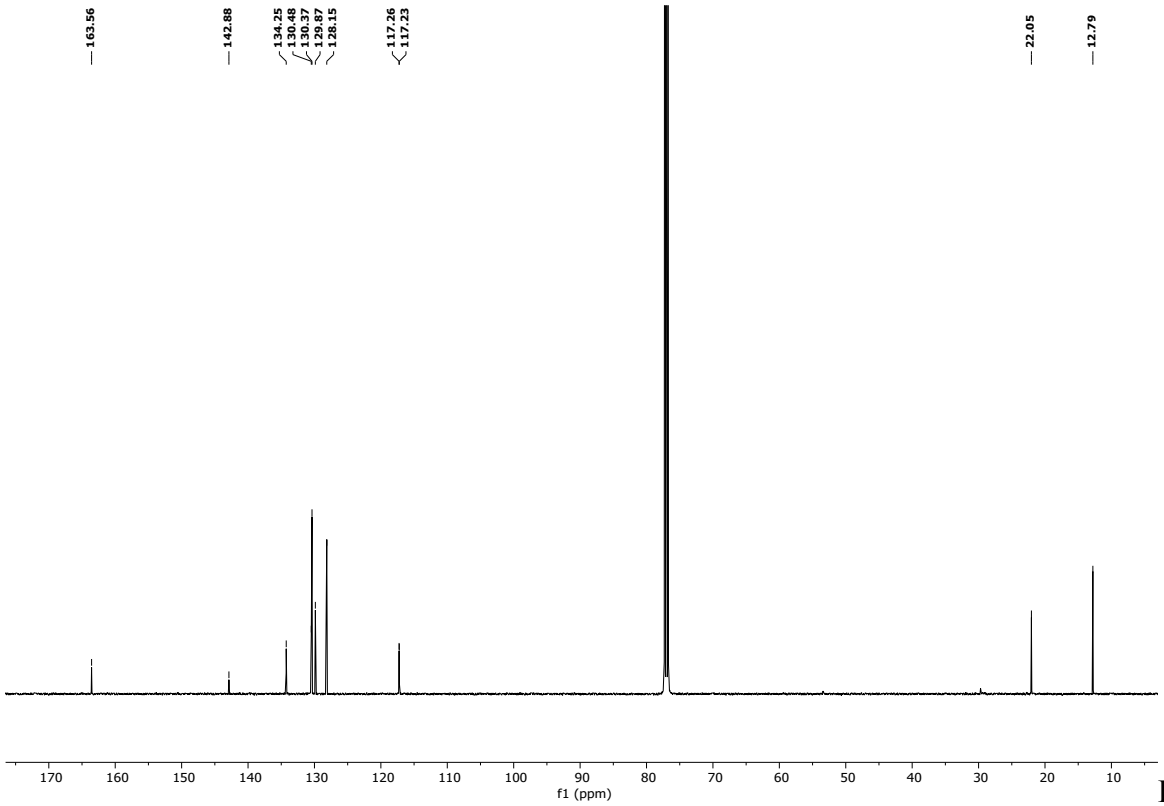

Figure S2: ^{13}C NMR Spectrum of the Compound **B0**

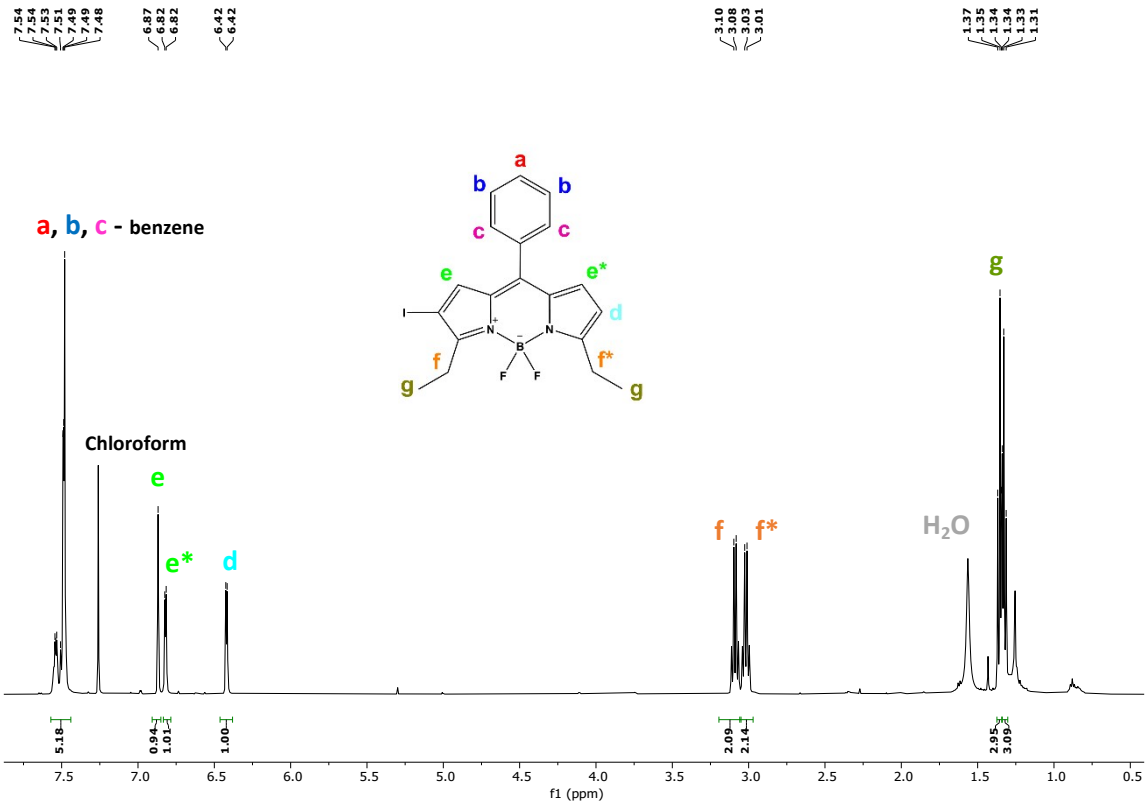

Figure S3: ^{1}H NMR Spectrum of the Compound **B1**

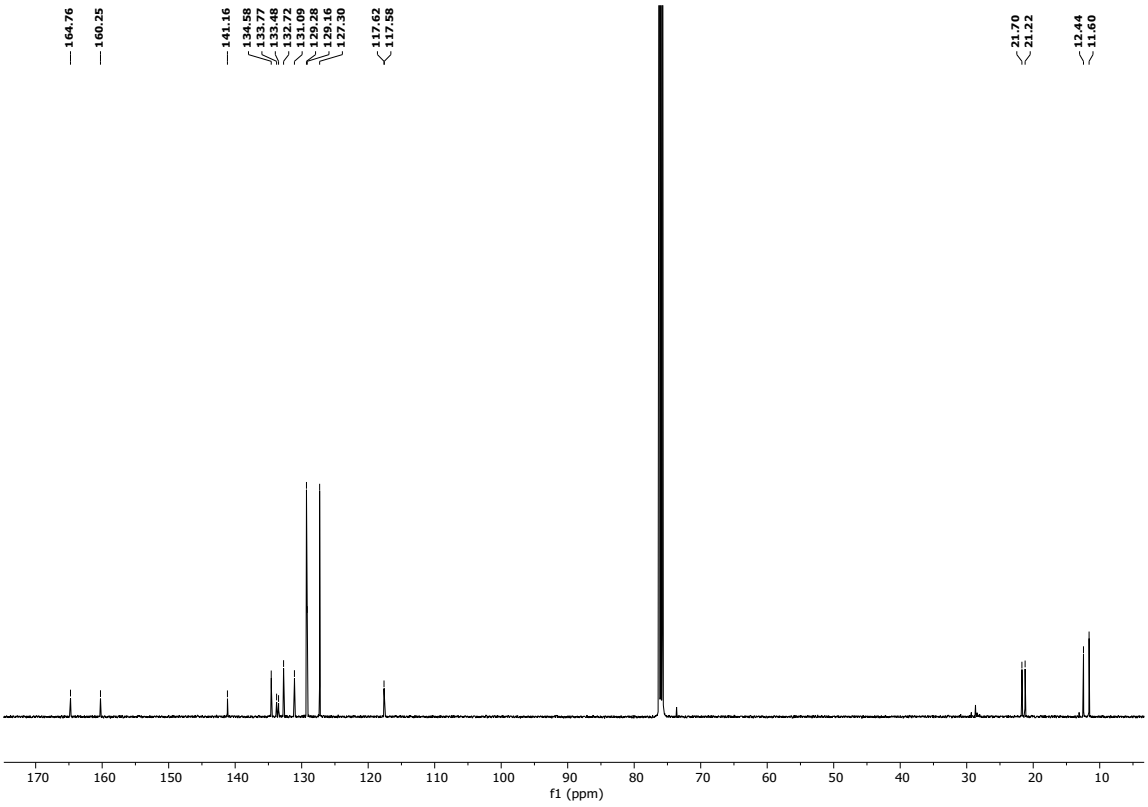

Figure S4: ^{13}C NMR Spectrum of the Compound **B1**

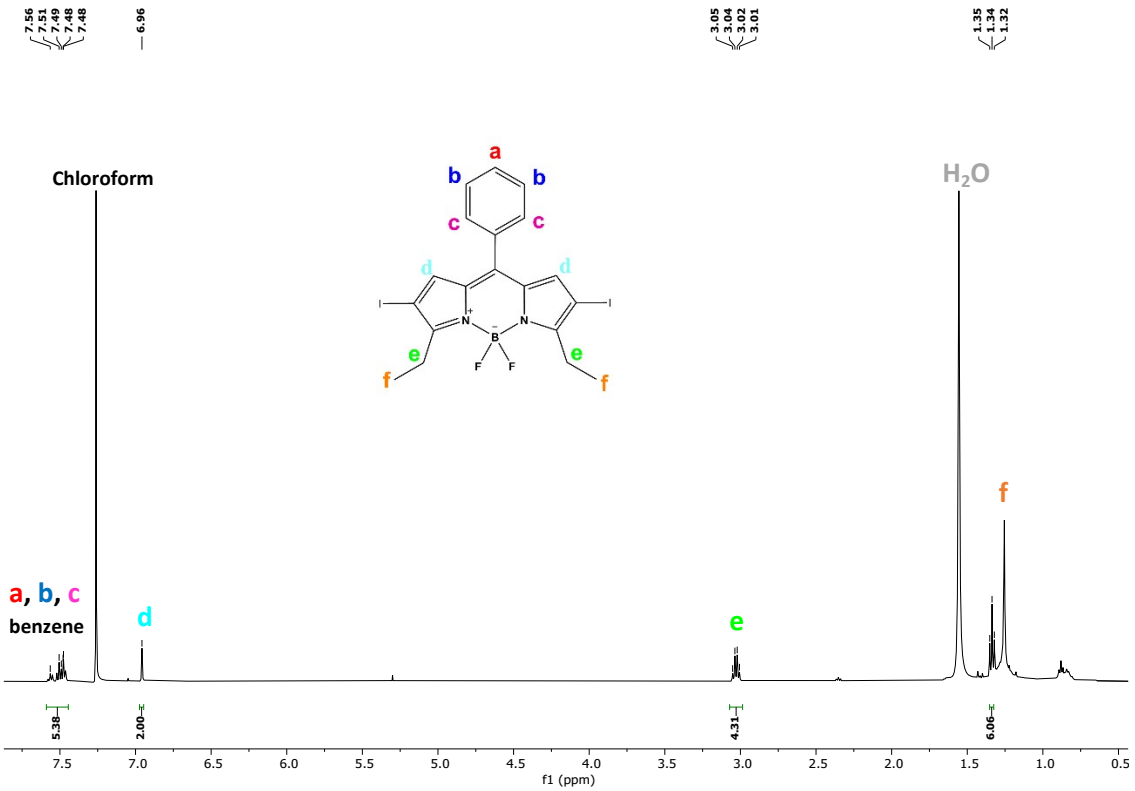

Figure S5: ^{1}H NMR Spectrum of the Compound **B2**

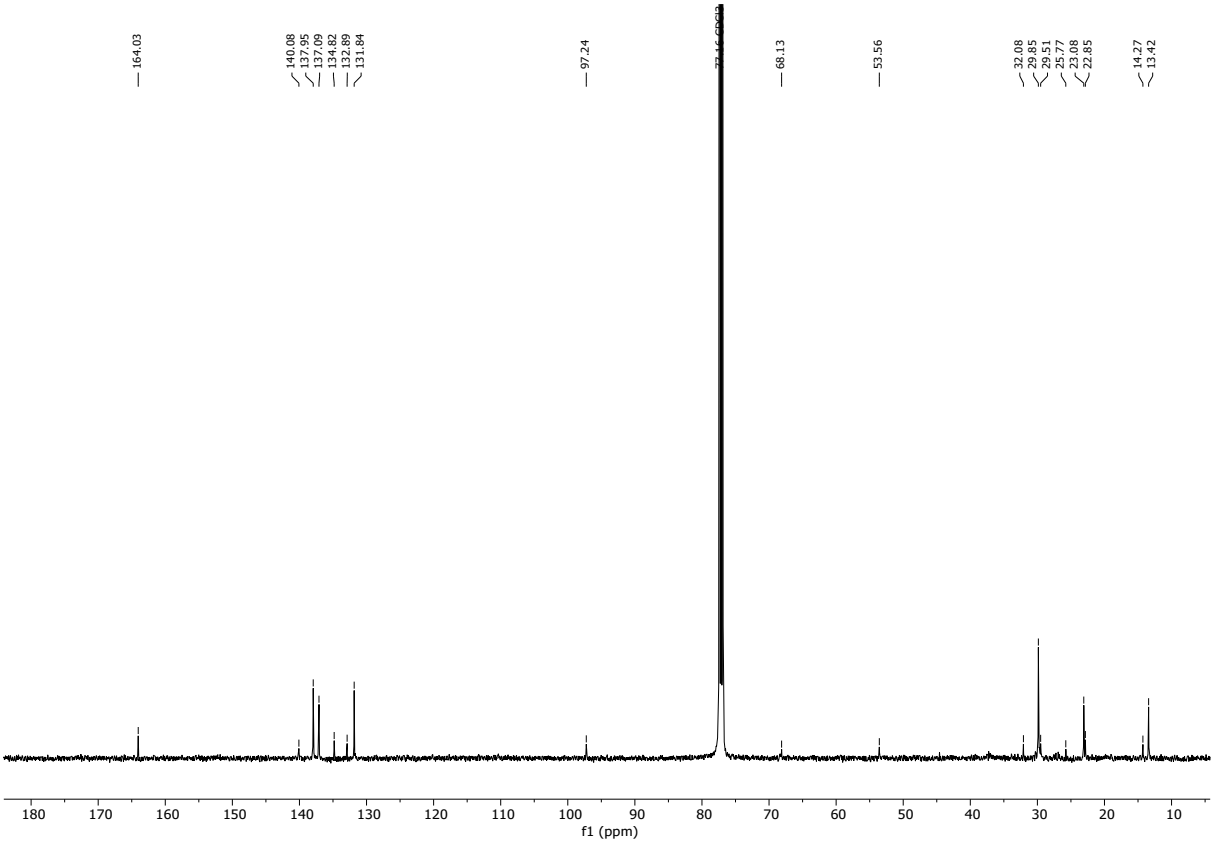

Figure S6: ^{13}C NMR Spectrum of the Compound **B2**

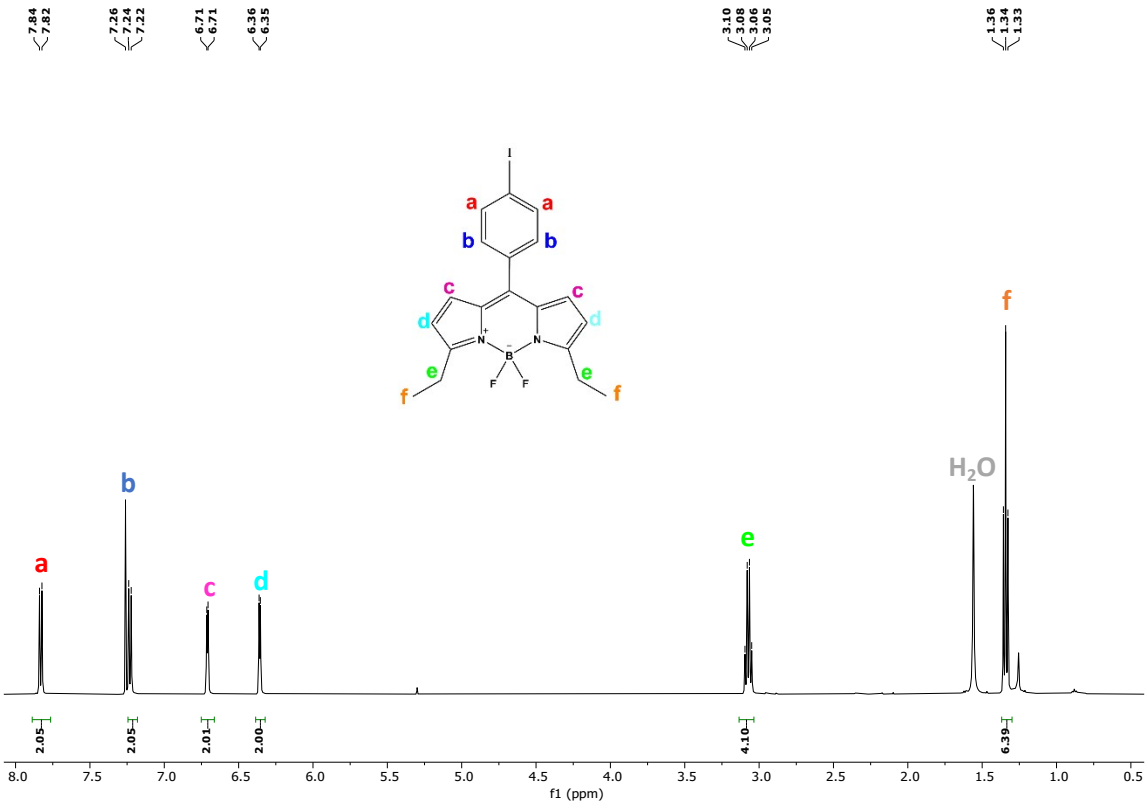

Figure S7: ^{1}H NMR Spectrum of the Compound **B3**

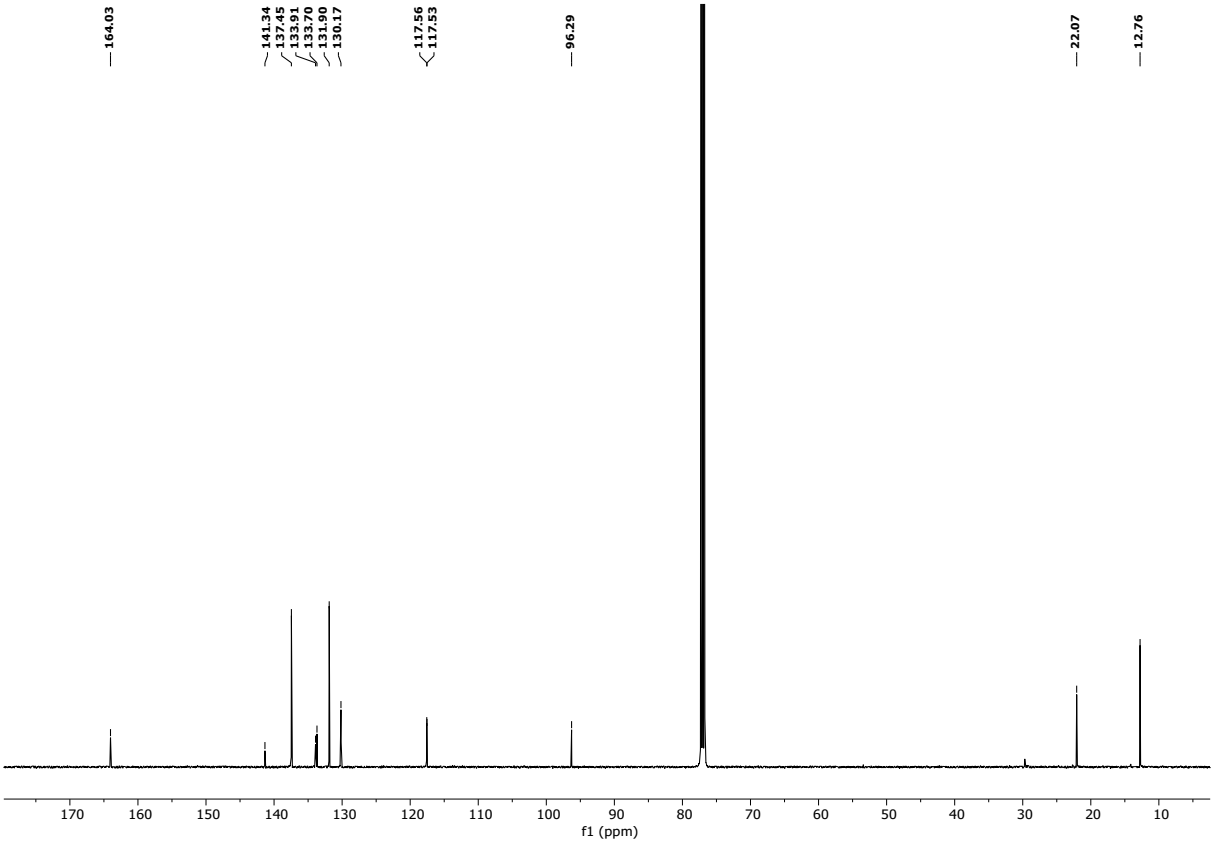

Figure S8: ^{13}C NMR Spectrum of the Compound **B3**

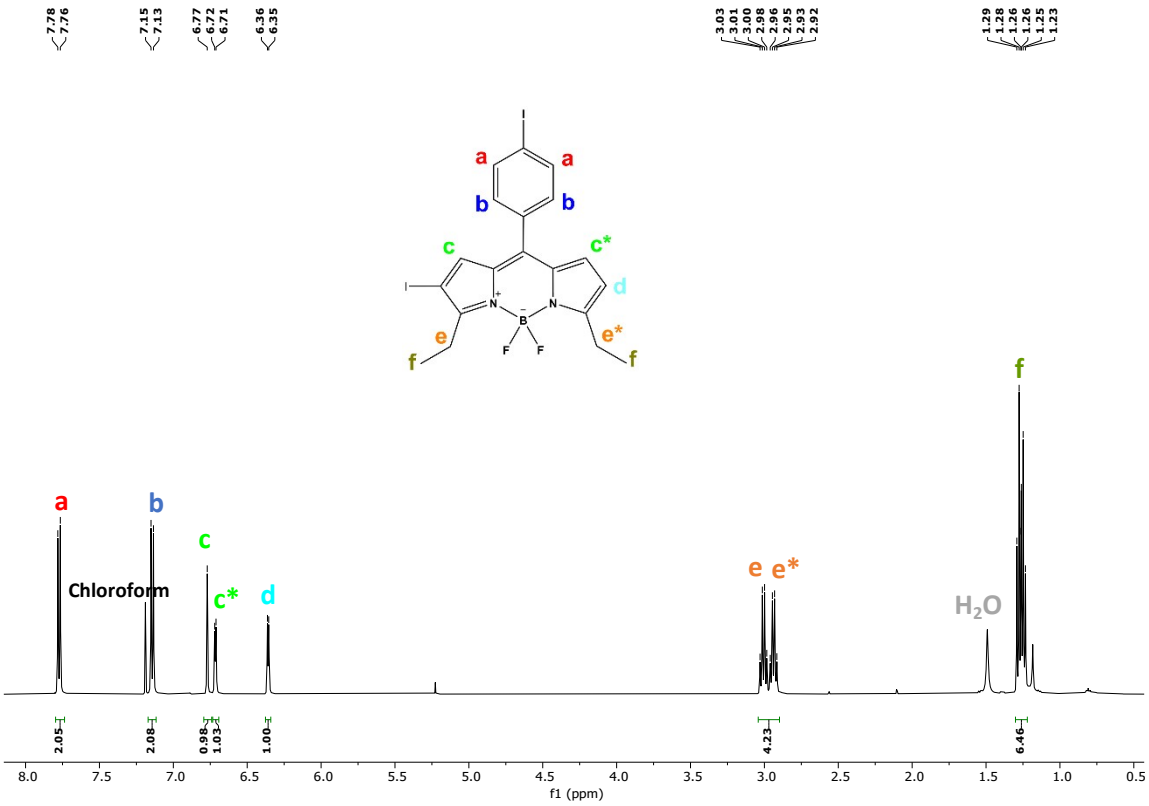

Figure S9: ^{1}H NMR Spectrum of the Compound **B4**

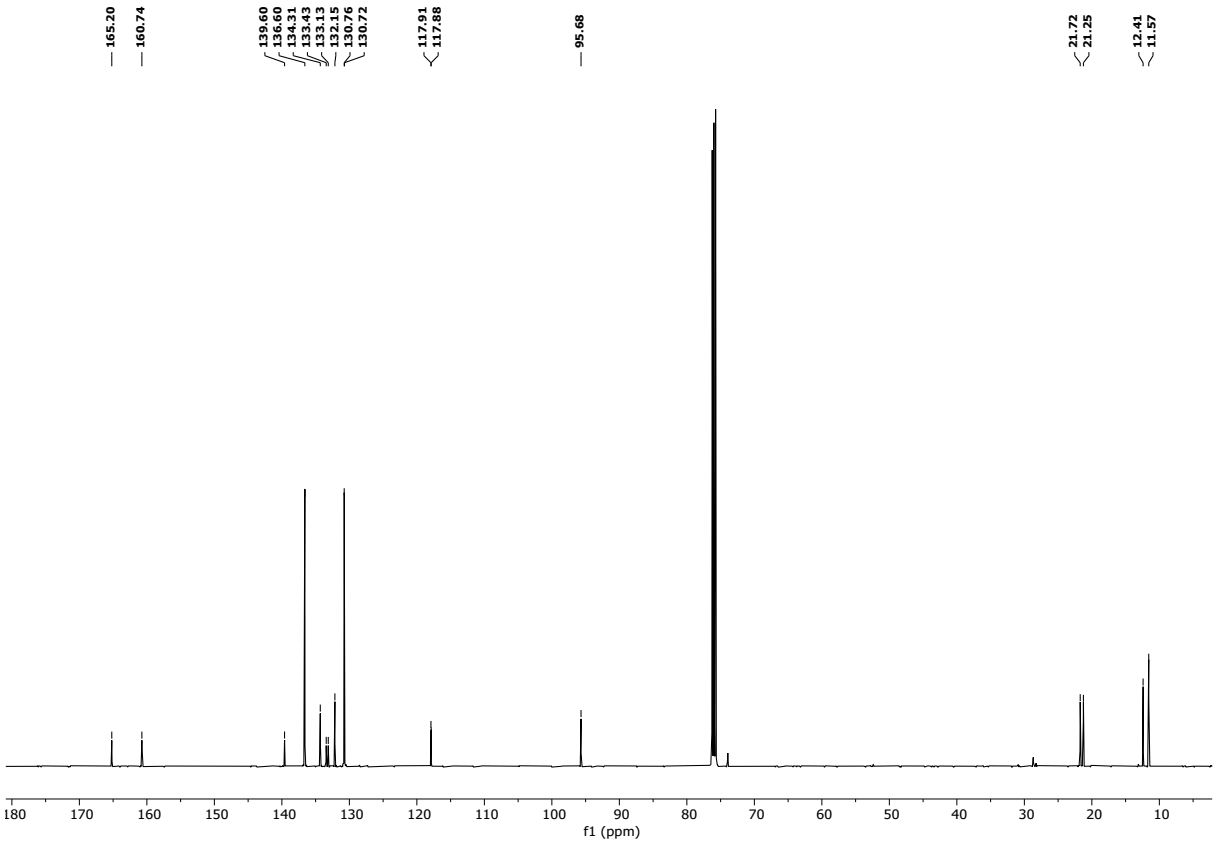

Figure S10: ^{13}C NMR Spectrum of the Compound **B4**

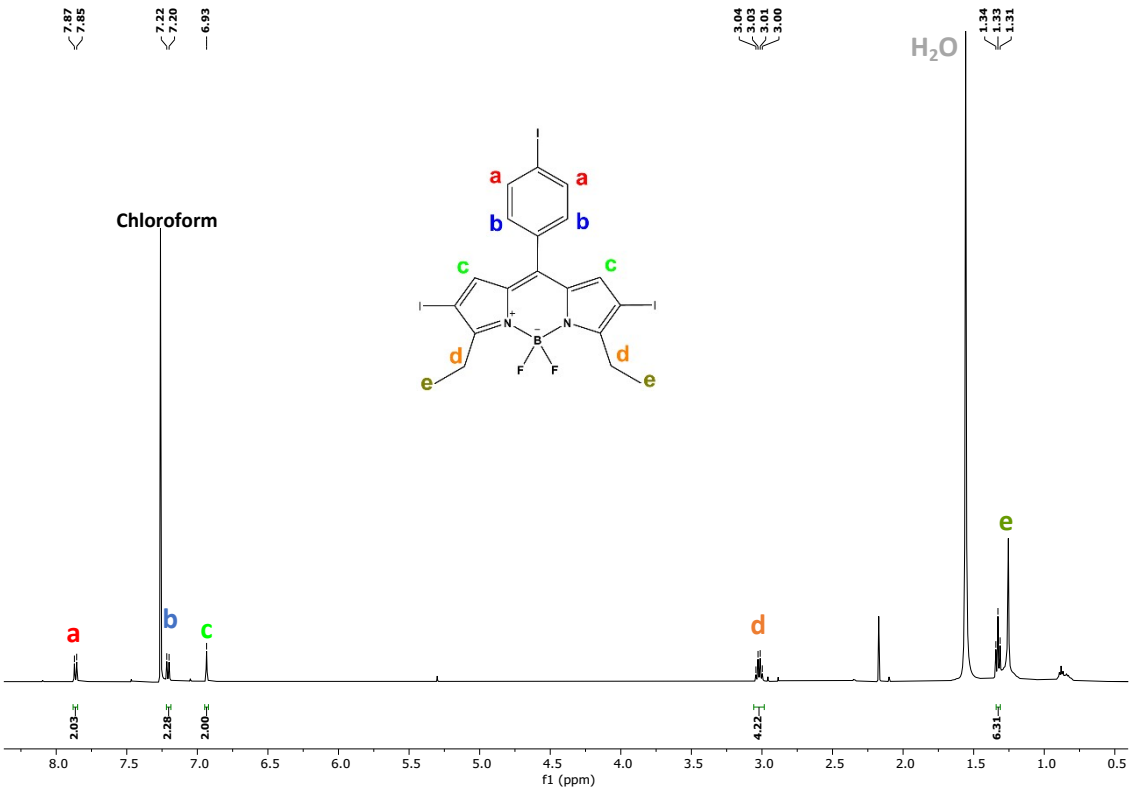

Figure S11: ^{1}H NMR Spectrum of the Compound **B5**

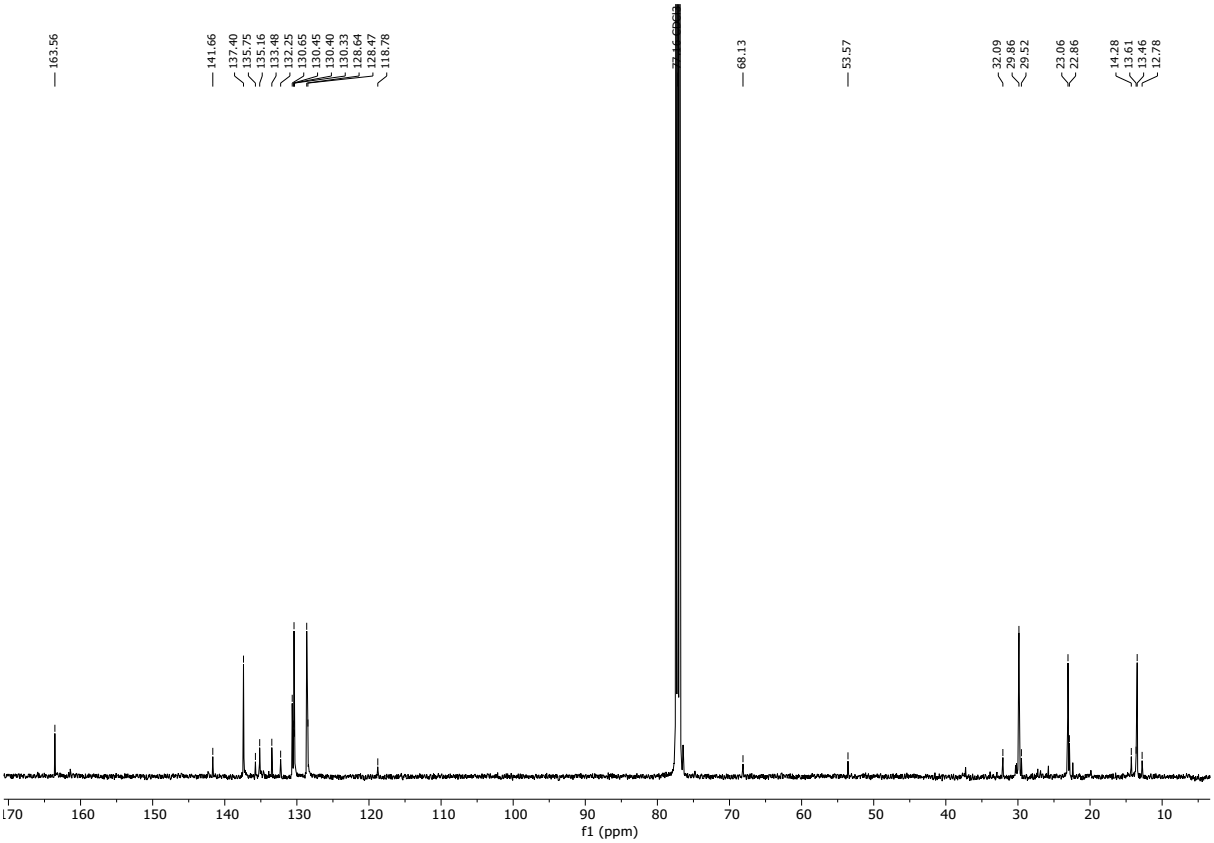

Figure S12: ^{13}C NMR Spectrum of the Compound **B5**

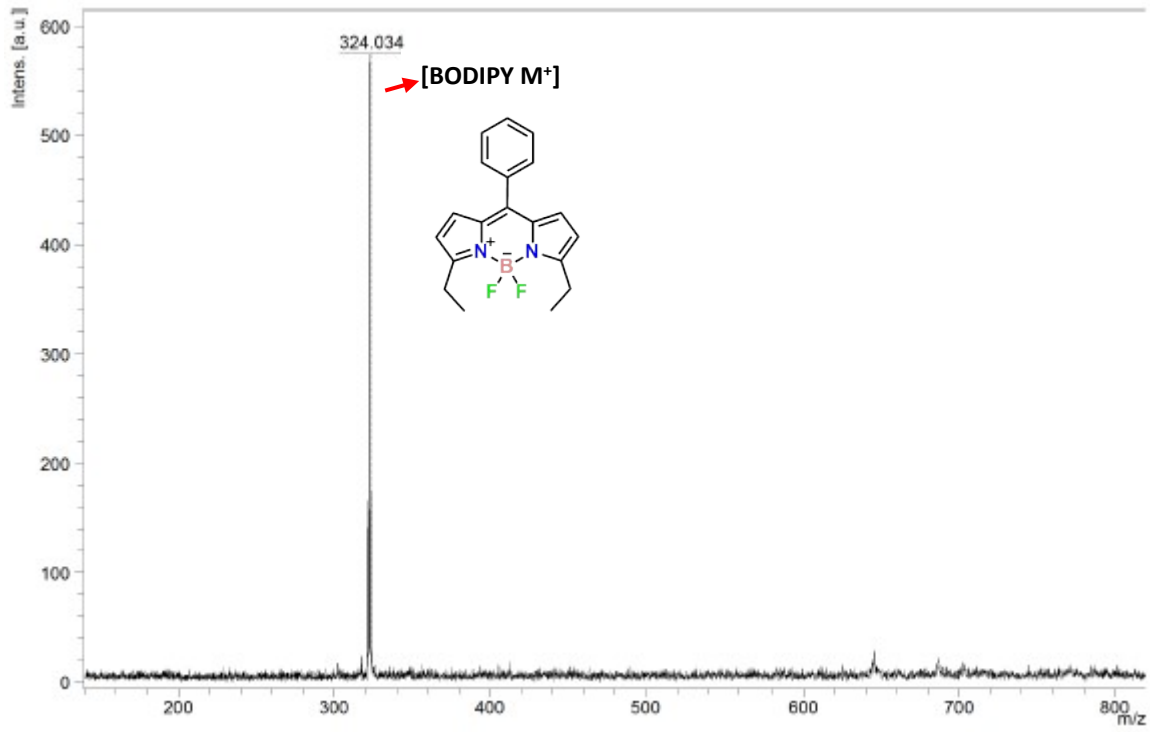

Figure S13: Mass Spectrum of Compound **B0**

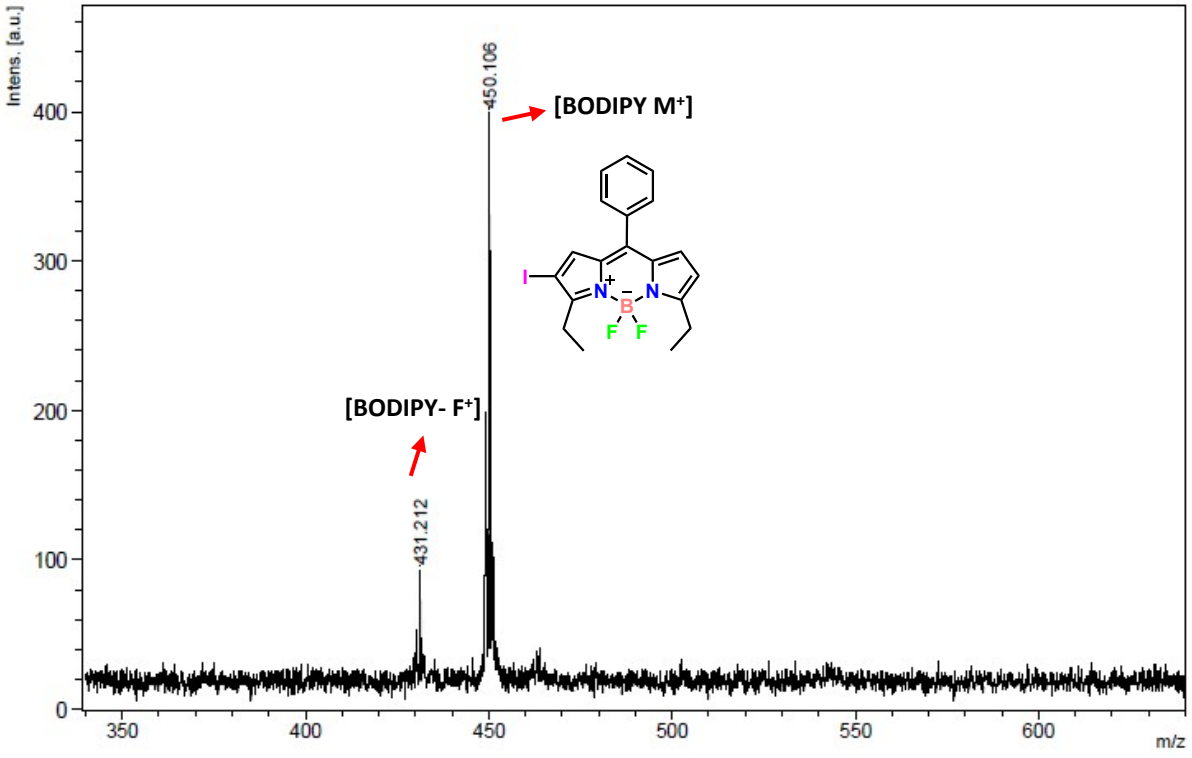

Figure S14: Mass Spectrum of Compound **B1**

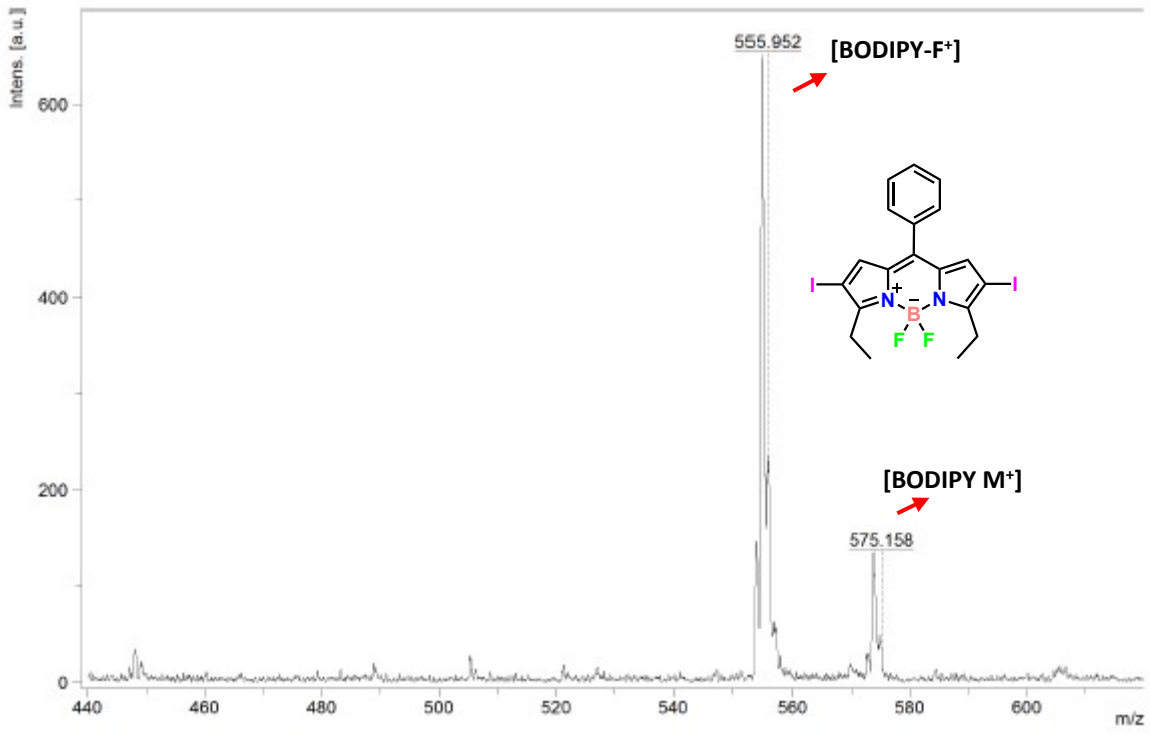

Figure S15: Mass Spectrum of Compound **B2**

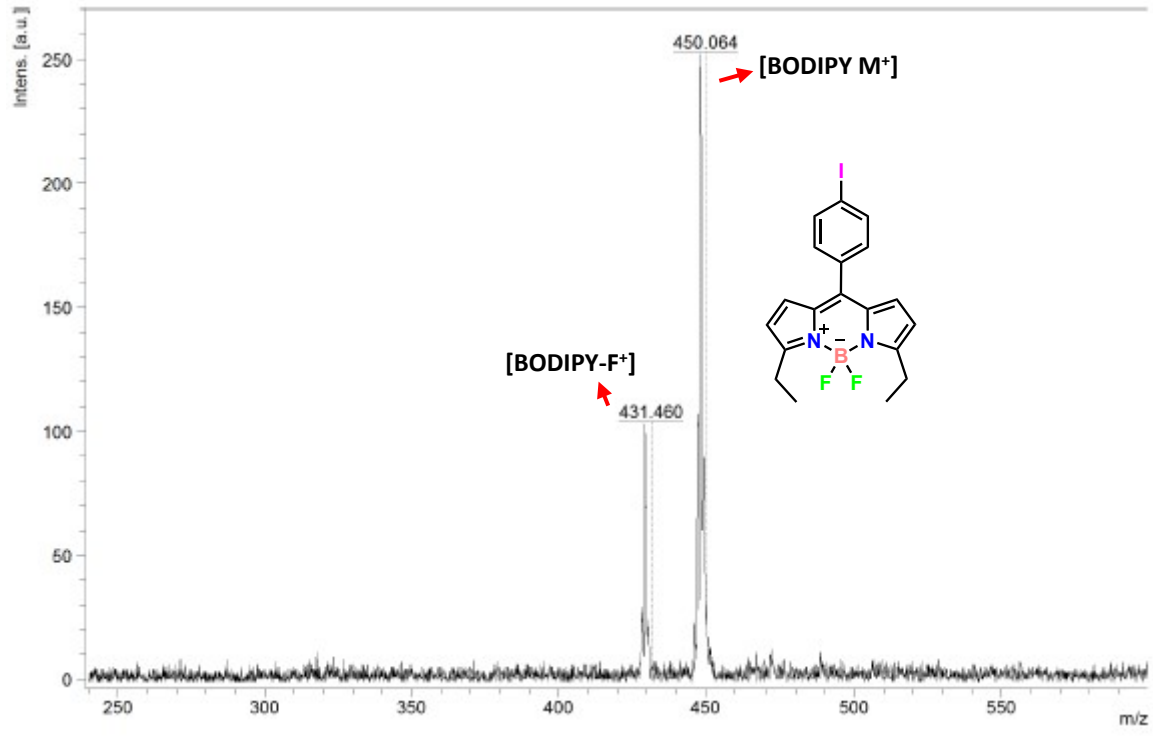

Figure S16: Mass Spectrum of Compound **B3**

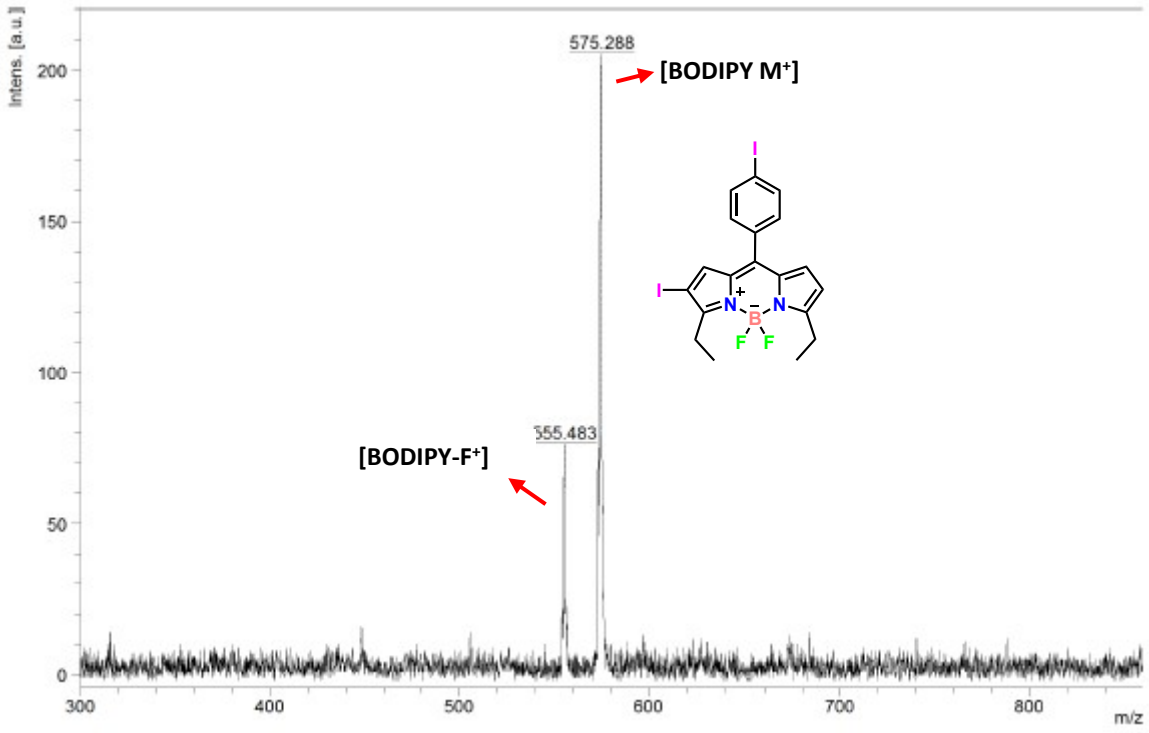

Figure S17: Mass Spectrum of Compound **B4**

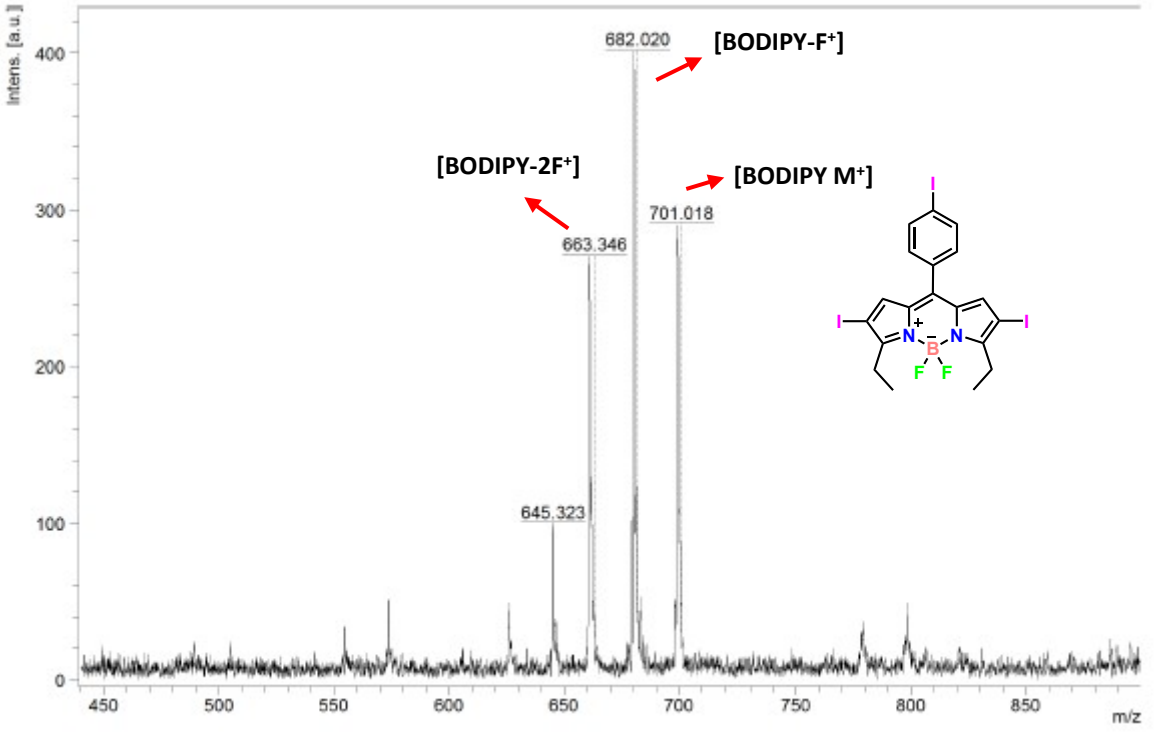

Figure S18: Mass Spectrum of Compound **B5**

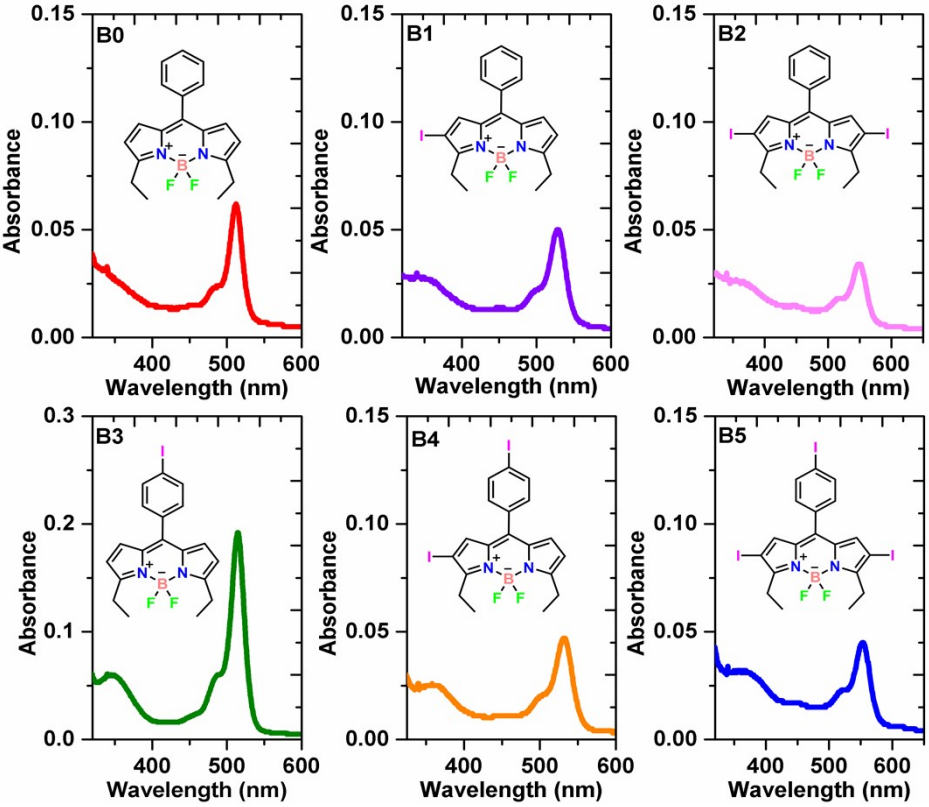

Figure S19: Absorption spectra of synthesized compounds (**B0-B5**) in DCM ($2x10^{-6}$M).

Table S1: Spectral data based on absorption measurements in DCM

Compounds	λ_{abs} (nm)	ε (10^5 M^{-1} cm^{-1})
B0	**512**	**1.60**
B1	**529**	**1.36**
B2	**550**	**0.93**
B3	**515**	**0.67**
B4	**533**	**0.64**
B5	**557**	**1.54**

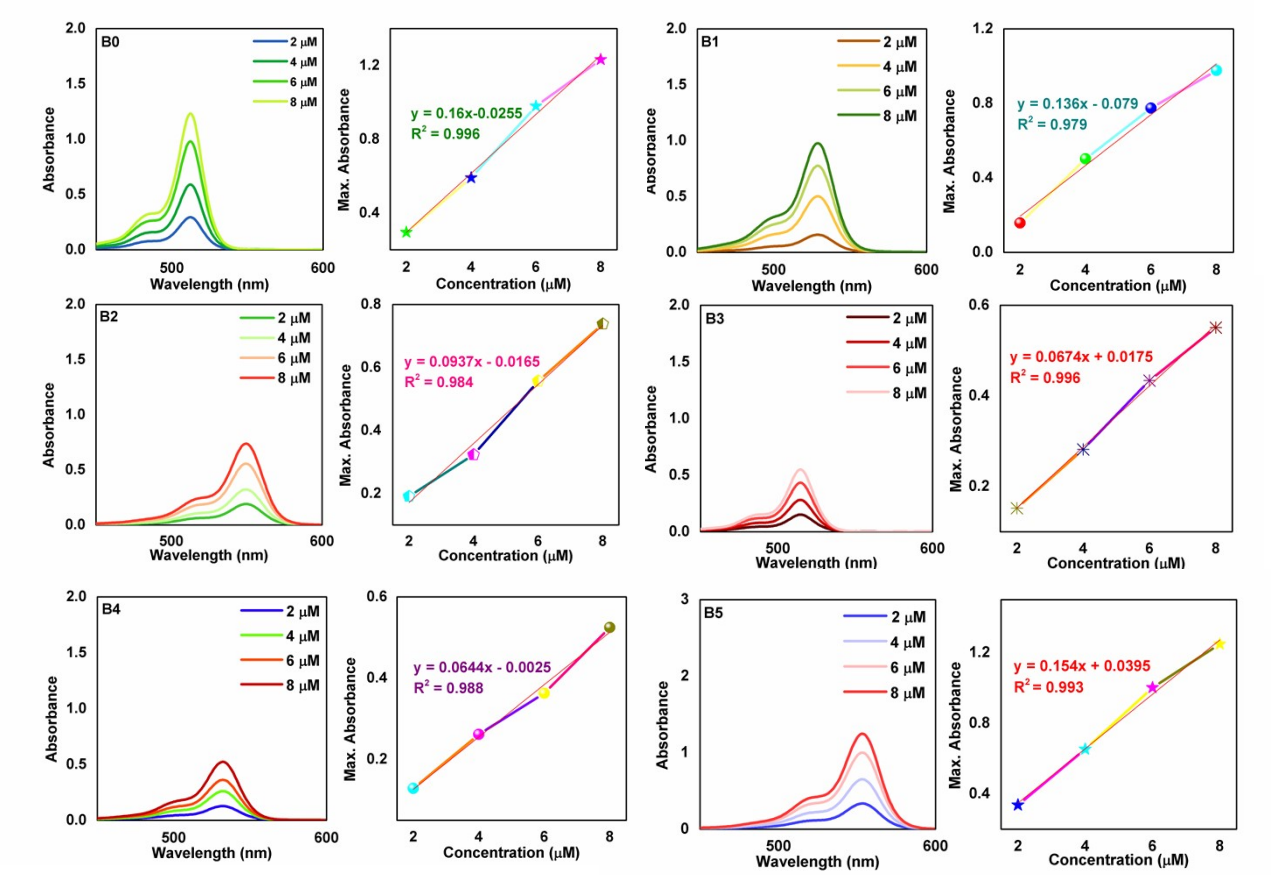

Figure S20: Absorbance spectrums of synthesized compounds at different concentrations.

Table S2. Crystal data and structure refinement details for **B1-B5**.

Compound	B1	B2	B3_	B4	B5
CCDC	2108982	2108984	2108981	2108983	2108985
Empirical formula	$C_{19}H_{18}BF_2IN_2$	$C_{19}H_{17}BF_2I_2N_2$	$C_{19}H_{18}BF_2IN_2$	$C_{19}H_{17}BF_2I_2N_2$	$C_{19}H_{16}BF_2I_3N_2$
Formula weight	450.06	575.96	450.06	575.96	701.85
Temperature/K	298	296	298	298	296
Radiation, Wavelength (Å)	MoKα (λ = 0.71073)	MoKα (λ = 0.71073)	MoKα (λ = 0.71073)	MoKα (λ = 0.71073)	MoKα (λ = 0.71073)
Crystal system	Triclinic	Monoclinic	Orthorhombic	Monoclinic	Orthorhombic
Space group	*P-1*	*C*2/*c*	$C222_1$	$P2_1/c$	*Pbcn*
a/Å	6.649(2)	36.279(7)	12.8973(11)	14.782(6)	10.7772(15)
b/Å	10.479(4)	6.3131(10)	13.3290(11)	10.554(4)	13.5103(19)
c/Å	14.000(5)	17.888(3)	10.5740(9)	13.415(6)	15.027(2)
α/°	106.646(8)	90	90	90	90
β/°	96.659(8)	104.391(13)	90	107.167(7)	90
γ/°	97.135(8)	90	90	90	90
Crystal size/mm³	0.12 × 0.07 × 0.05	0.27 × 0.14 × 0.12	0.19 × 0.12 × 0.08	0.15 × 0.11 × 0.05	0.17 × 0.14 × 0.08
Volume/Å³	915.4(6)	3968.5(12)	1817.8(3)	1999.6(14)	2188.0(6)
Z	2	8	4	4	4
ρ_{calc}g/cm³	1.633	1.928	1.645	1.913	2.131
μ/mm⁻¹)	1.771	3.193	1.784	3.168	4.308
***F*(000)**	444	2192	888	1096	1304
2θ range for data collection/°	3.076 to 50	2.318 to 50	4.394 to 50	2.884 to 50	4.834 to 50
Index ranges	-7 ≤ h ≤ 7, -12 ≤ k ≤ 12, -16 ≤ l ≤ 16	-42 ≤ h ≤ 41, 0 ≤ k ≤ 7, 0 ≤ l ≤ 21	-15 ≤ h ≤ 15, -15 ≤ k ≤ 15, -12 ≤ l ≤ 12	-17 ≤ h ≤ 15, -11 ≤ k ≤ 12, -13 ≤ l ≤ 15	-12 ≤ h ≤ 10, -16 ≤ k ≤ 12, -17 ≤ l ≤ 12
Reflections collected	9330	3436	6835	8789	8067
Independent reflections	9330	3436 [Rint = ?, R_{sigma} = 0.0900]	1609	3510 [R_{int} = 0.0416, R_{sigma} = 0.0516]	1930 [Rint = 0.0328, Rsigma = 0.0283]
Data/restraints/parameters	9330/54/229	3436/66/238	1609/0/117	3510/0/237	1930/0/126
Goodness-of-fit on F^2 (S)	1.043	1.042	1.016	1.023	1.034
Final R indices [$I > 2\sigma(I)$]	R_1 = 0.0729, wR_2 = 0.1908	R_1 = 0.0556, wR_2 = 0.1069	R_1 = 0.0274, wR_2 = 0.0666	R_1 = 0.0415, wR_2 = 0.0857	R_1 = 0.0293, wR_2 = 0.0656
R indices (all data)	R_1 = 0.1148, wR_2 = 0.2136	R_1 = 0.1133, wR_2 = 0.1267	R_1 = 0.0305, wR_2 = 0.0680	R_1 = 0.0682, wR_2 = 0.0974	R_1 = 0.0364, wR_2 = 0.0698
Largest diff. peak/hole / e Å⁻³	1.03/-1.08	1.13/-1.73	0.26/-0.55	1.25/-0.79	1.11/-1.18

Table S3. Selected bond lengths (Å) and bond angles (°) for BODIPY derivatives.

Bond Distances (Å)	B1	B2	B3	B4	B5
F1—B1	1.370 (18)	1.365 (17)	1.383 (4)	1.375 (8)	1.387 (4)
F2—B1	1.376 (16)	1.394 (17)	-	1.371 (8)	-
N1—B1	1.547 (17)	1.549 (17)	1.559 (5)	1.547 (9)	1.564 (5)
N2—B1	1.543 (17)	1.540 (18)	-	1.553 (8)	-
N1—C1	1.359 (15)	1.364 (15)	1.351 (6)	1.353 (8)	1.361 (5)
N1—C4	1.420 (14)	1.414 (15)	1.396(6)	1.399 (7)	1.412 (5)
Dihedral Angles (°)	68.59	60.50	58.78	61.57	60.82
Bond Angles (°)					
F1—B1—F2/F1^{i}	108.6 (12)	109.5 (8)	109.7 (4)	109.3 (5)	109.8 (5)
F1—B1—N1	110.6 (12)	111.4 (13)	110.15 (18)	110.2 (5)	109.88 (17)
F1—B1—N2/N1^{i}	110.4 (10)	112.3 (13)	109.84 (18)	110.2 (5)	110.27 (16)
F2/F1^{i}—B1—N1	109.6 (10)	107.9 (13)	109.84 (18)	110.0 (6)	110.27 (16)
F2/F1^{i}—B1—N2/N1^{i}	110.2 (12)	108.8 (13)	110.15 (18)	110.6 (5)	109.87 (17)
N2/N1^{i}—B1—N1	107.5 (11)	106.8 (7)	107.2 (4)	106.5 (5)	106.7 (4)
C1—N1—B1	127.6 (11)	126.7 (10)	127.1 (4)	127.6 (5)	126.8 (3)
C4—N1—B1	124.0 (10)	125.2 (11)	124.4 (4)	125.0 (5)	125.3 (3)
C6—N2—B1	124.7 (10)	125.2 (11)	-	124.3 (5)	-
C9—N2—B1	127.3 (10)	128.2 (10)	-	127.2 (5)	-

For **B3**: Symmetry code: (i) −x+1, y, −z+1/2, for **B5**: Symmetry code: (i) −x+1, y, −z+3/2.

Table S4. Halogen bonding parameters for BODIPY derivatives.

Bond Distances (Å)	B1	B2	B3	B4	B5
F1—B1	1.370 (18)	1.365 (17)	1.383 (4)	1.375 (8)	1.387 (4)
F2—B1	1.376 (16)	1.394 (17)	-	1.371 (8)	-
N1—B1	1.547 (17)	1.549 (17)	1.559 (5)	1.547 (9)	1.564 (5)
N2—B1	1.543 (17)	1.540 (18)	-	1.553 (8)	-
N1—C1	1.359 (15)	1.364 (15)	1.351 (6)	1.353 (8)	1.361 (5)
N1—C4	1.420 (14)	1.414 (15)	1.396(6)	1.399 (7)	1.412 (5)
Dihedral Angles (°)	68.59	60.50	58.78	61.57	60.82
Bond Angles (°)					
F1—B1—F2/F1^{i}	108.6 (12)	109.5 (8)	109.7 (4)	109.3 (5)	109.8 (5)
F1—B1—N1	110.6 (12)	111.4 (13)	110.15 (18)	110.2 (5)	109.88 (17)
F1—B1—N2/N1^{i}	110.4 (10)	112.3 (13)	109.84 (18)	110.2 (5)	110.27 (16)
F2/F1^{i}—B1—N1	109.6 (10)	107.9 (13)	109.84 (18)	110.0 (6)	110.27 (16)
F2/F1^{i}—B1—N2/N1^{i}	110.2 (12)	108.8 (13)	110.15 (18)	110.6 (5)	109.87 (17)
N2/N1^{i}—B1—N1	107.5 (11)	106.8 (7)	107.2 (4)	106.5 (5)	106.7 (4)
C1—N1—B1	127.6 (11)	126.7 (10)	127.1 (4)	127.6 (5)	126.8 (3)
C4—N1—B1	124.0 (10)	125.2 (11)	124.4 (4)	125.0 (5)	125.3 (3)
C6—N2—B1	124.7 (10)	125.2 (11)	-	124.3 (5)	-
C9—N2—B1	127.3 (10)	128.2 (10)	-	127.2 (5)	-

For **B3**: Symmetry code: (i) −x+1, y, −z+1/2, for **B5**: Symmetry code: (i) −x+1, y, −z+3/2.

Table S5. The intermolecular C-H···F interactions (Å and °) for **BODIPY** derivatives.

D-H···A	Symmetry	d(D-H)	d(H···A)	d(D-H···A)	D-H···A
B1					
C16-H16A···F2	1+x, y, z	0.97	2.58	3.516	161
B2					
C16-H16B···F1	x, -1+y, z	0.97	2.44	3.355	157
C18-H18B···F2	x, 1+y, z	0.97	2.50	3.415	156
B3					
C8-H8B···F1	x, 1-y, 1-z	0.93	2.53	3.393	159
B4					
C11-H11···F1	x, 1/2-y, -1/2+z	0.93	2.67	3.271	123
C12-H12···F1	x, 1/2-y, -1/2+z	0.93	2.62	3.240	125

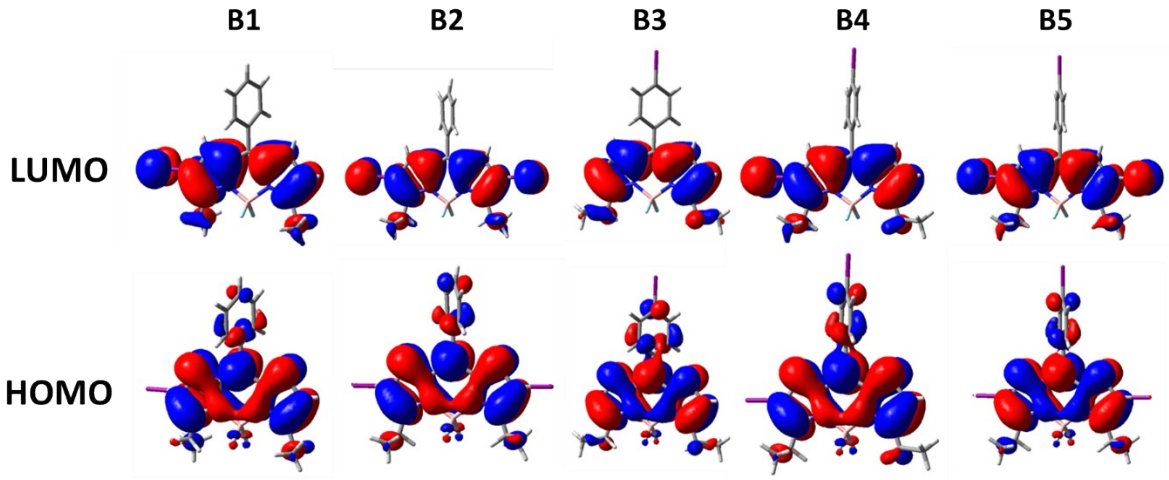

Figure S21. Molecular orbital plots of the HOMOs and LUMOs of **B1-B5.**

Table S6. Electron density (ρ,au), Laplacian ($\Delta^2\rho$, au) and energy density (H, au) at the intermolecular bond critical points in the **B1-B5** dimers

Dimers	Interaction	ρ	$\nabla^2\rho$	H
B1-I	I··· π_{BODIPY}	0.00580	0.01515	0.00056
	HC···F	0.00580	0.02672	0.00128
	HC···F	0.00276	0.01338	0.00094
B1-II	I···π_{phenyl}	0.00739	0.02042	0.00082
	HC···I	0.00422	0.01281	0.00075
B2-I	I··· π_{BODIPY}	0.00517	0.01339	0.00053
	HC···I	0.00145	0.00454	0.00033
	HC···F	0.00703	0.03122	0.00127
	HC···F	0.00799	0.03490	0.00123
B2-IIa	I···I	0.00680	0.01815	0.00076
	HC···I	0.00597	0.01795	0.00092
B2-IIb	I···I	0.00602	0.01626	0.00073
	HC···I	0.00336	0.00976	0.00056
B3	I···F	0.00718	0.02732	0.00106
	HC···I	0.00370	0.01157	0.00070
B4-I	I···F	0.00876	0.03322	0.00107
	HC···I	0.00406	0.01289	0.00076
B4-II	I···I	0.01063	0.02722	0.00082
	HC···I	0.00342	0.01085	0.00065
B5-I	I···F	0.00570	0.02251	0.00104
	HC···I	0.00304	0.00968	0.00062
B5-II	I···I	0.00926	0.02378	0.00082
	HC···I	0.00306	0.00958	0.00058

Table S7. Summary of SAPT results of the **B1-B5** dimers.

Compound		E_{elst}	E_{exch}	E_{ind}	E_{disp}	E_{int}
B1-I	I···π_{BODIPY}	-5.2	11.3	-1.4	-20.5	**-15.8**
B1-II	I···π_{phenyl}	-7.1	13.1	-1.7	-15.0	**-10.7**
B2-I	I···π_{BODIPY}	-6.0	14.9	-2.0	-27.7	**-20.8**
B2-IIa	I···I ($d_{I1\cdots I2}$ = 3.976 Å)	-1.9	5.0	-0.8	-7.0	**-4.6**
B2-IIb	I···I ($d_{I1\cdots I2}$ = 4.043 Å)	-1.5	3.8	-0.6	-6.5	**-4.9**
B3	I···F	-3.0	4.6	-1.1	-5.1	**-4.5**
B4-I	I···F	-3.0	3.9	-0.9	-4.8	**-4.8**
B4-II	I···I	-3.3	7.0	-1.3	-6.0	**-3.6**
B5-I	I···F	-2.5	3.3	-0.7	-4.9	**-4.8**
B5-II	I···I	-2.7	5.5	-1.1	-5.4	**-3.6**

Hirshfeld Surface Analysis

Hirshfeld surfaces incorporating two-dimensional (2D) fingerprint plots using Crystal Explorer was used in order to get a better insight into the intermolecular interactions in the solid state of **B1-B5**.[3–5] The normalized contact distance (d_{norm}) surface, which expressed in terms of distances to the surface from the nuclei inside and outside the Hirshfeld surface (d_i, and d_e, respectively) and the vdW radii of the atoms, defined as Eq. 1 gives identification of the regions of particular importance to intermolecular interactions.[6,7] The 2D fingerprint plots for **B1**-**B5** (Figure S22-S26), which were derived from the combination of d_i, and d_e, were used for quantifying the intermolecular contacts in the crystal.

$$d_{norm} = \frac{d_i - r_i^{vdw}}{r_i^{vdw}} + \frac{d_e - r_e^{vdw}}{r_e^{vdw}} \qquad \text{Equation (1)}$$

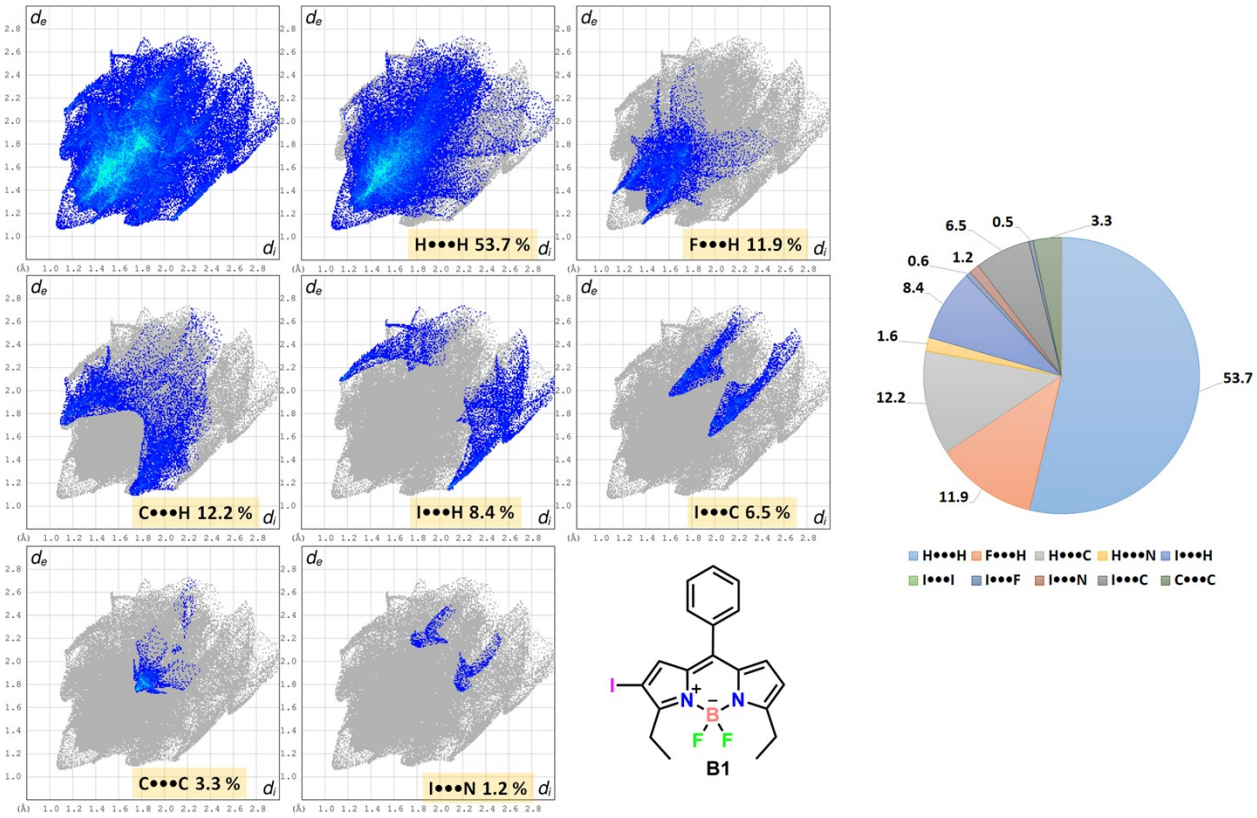

Figure S22. Full fingerprint plots and the resolved fingerprint plots showing the percentage contributions to the total Hirshfeld surface area in **B1**.

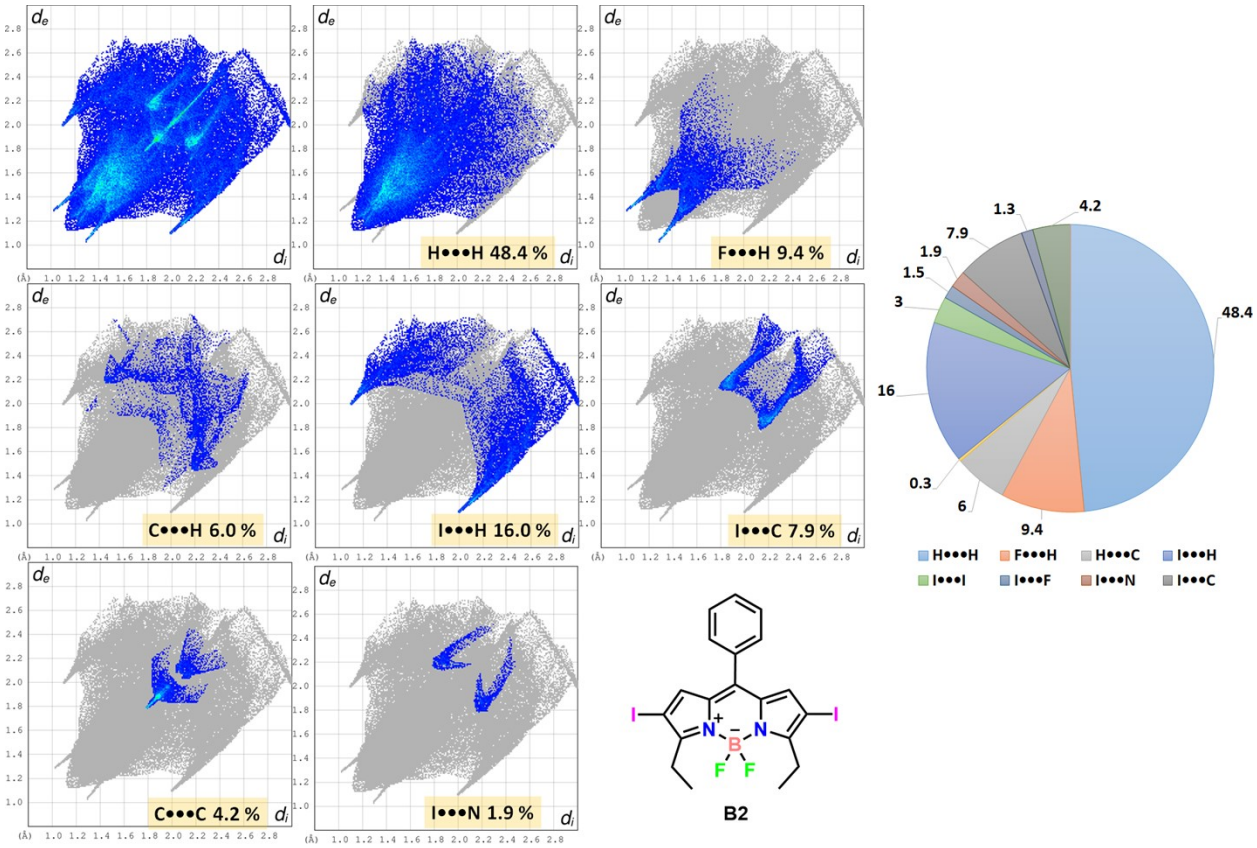

Figure S23. Full fingerprint plots and the resolved fingerprint plots showing the percentage contributions to the total Hirshfeld surface area in **B2**.

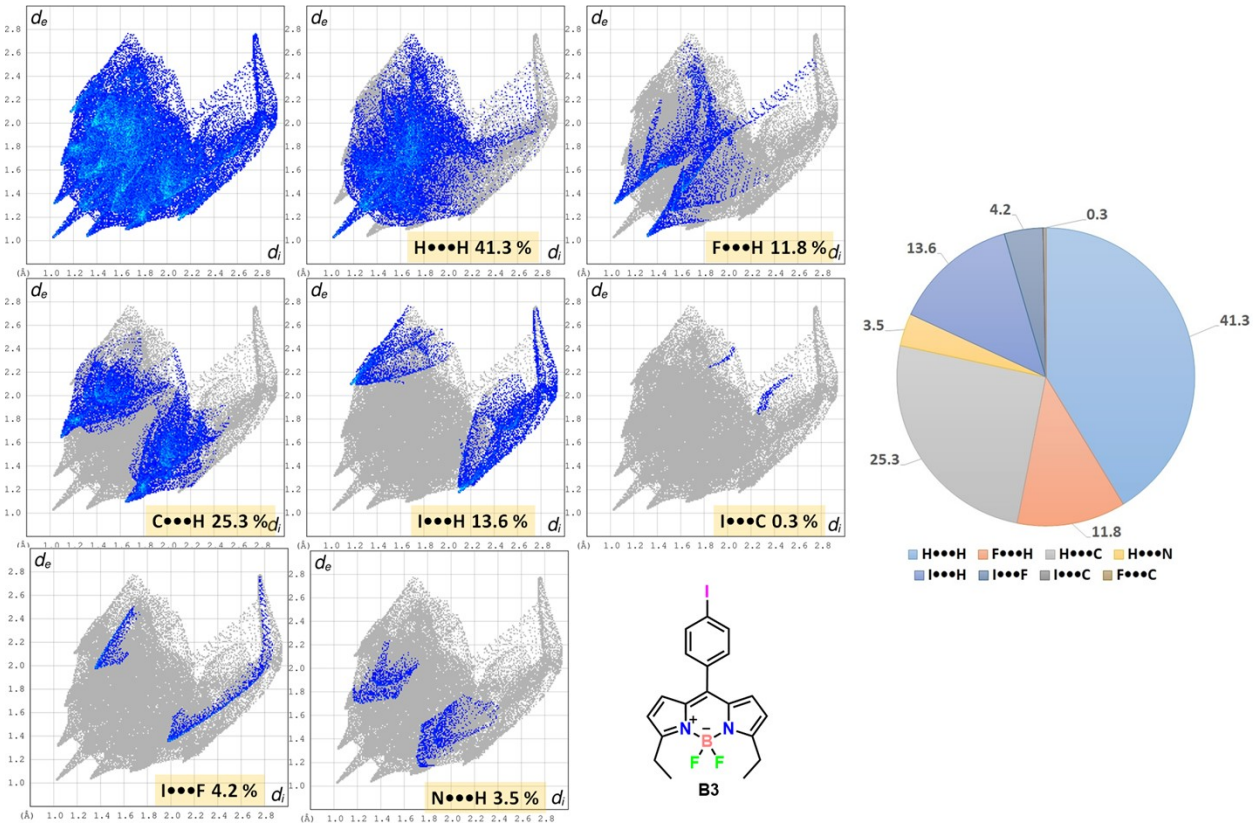

Figure S24. Full fingerprint plots and the resolved fingerprint plots showing the percentage contributions to the total Hirshfeld surface area in **B3**.

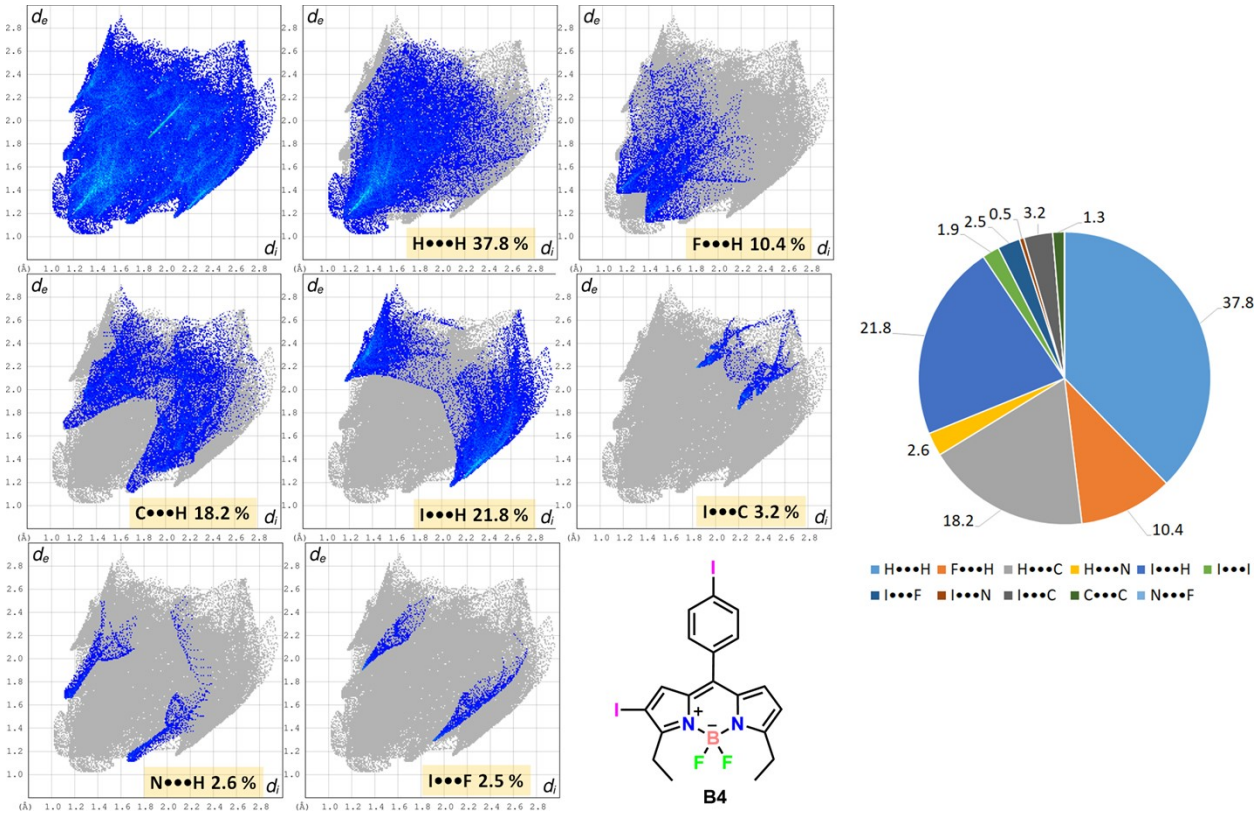

Figure S25. Full fingerprint plots and the resolved fingerprint plots showing the percentage contributions to the total Hirshfeld surface area in **B4**.

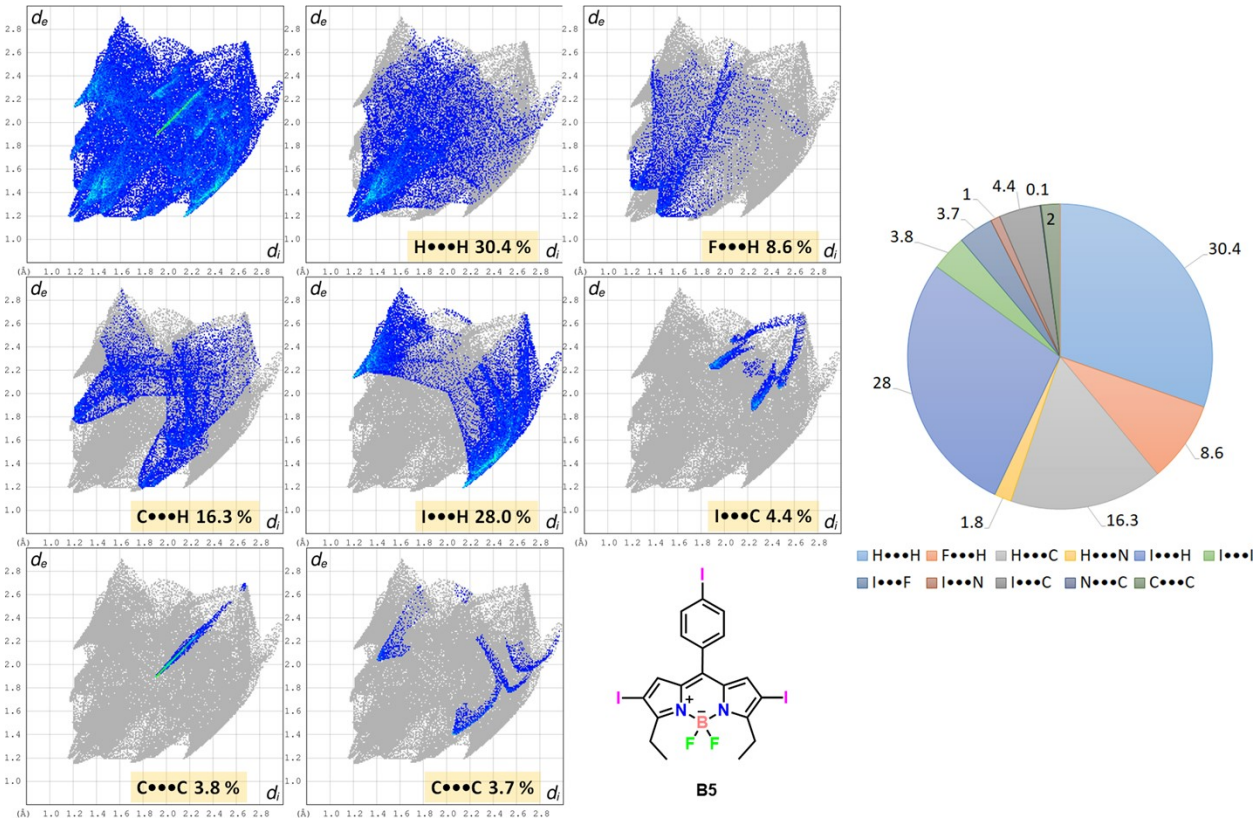

Figure S26. Full fingerprint plots and the resolved fingerprint plots showing the percentage contributions to the total Hirshfeld surface area in **B5**.

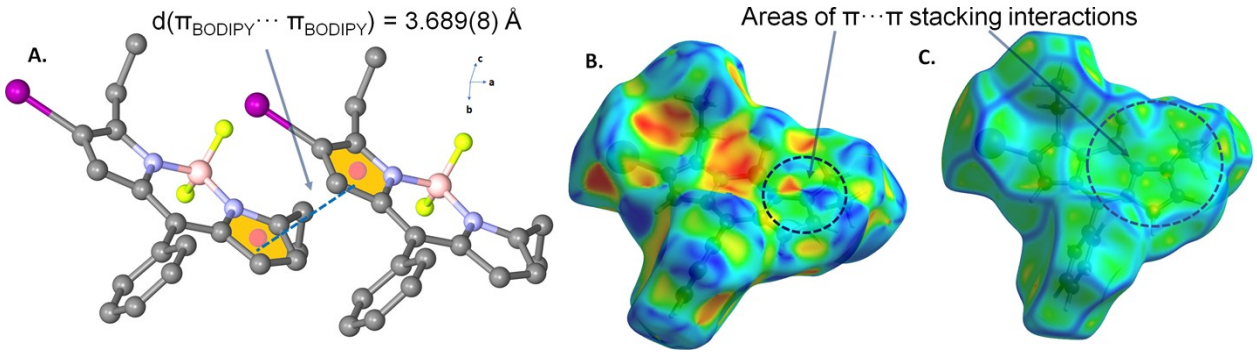

Figure S27. A) The $\pi_{BODIPY}\cdots\pi_{BODIPY}$ interaction between the pyrrole moiety of BODIPY B) and C) Hirshfeld surfaces of **B1** mapped with shape index and curvedness. Areas of π···π stacking interactions are highlighted as yellow dashed circles.

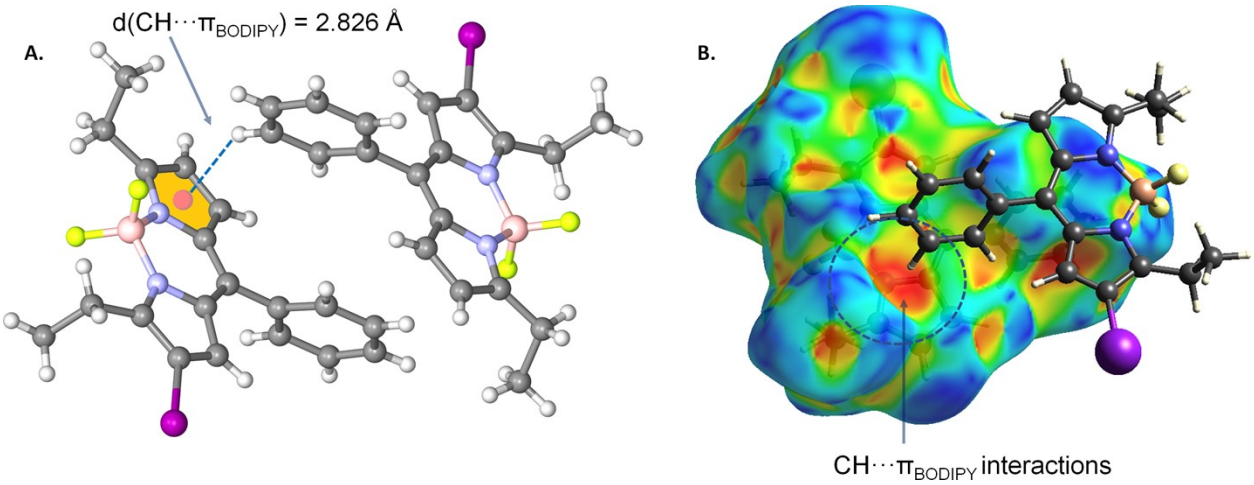

Figure S28 A) The CH···π_{BODIPY} interaction in **B1**. B) and C) Hirshfeld surfaces of **B1** mapped with shape index, showing areas of CH···π stacking interactions highlighted as black dashed circles.

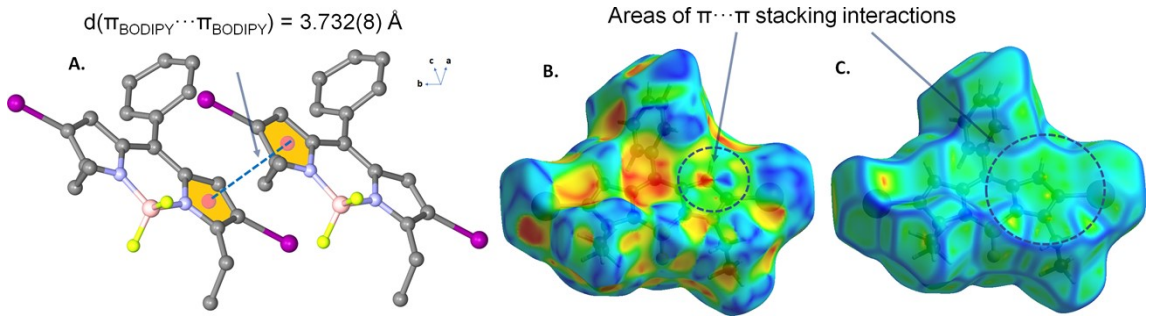

Figure S29. A) The π_{BODIPY}···π_{BODIPY} interaction between the pyrrole moiety of BODIPY. B) and C) Hirshfeld surfaces of **B2** mapped with shape index and curvedness. Areas of π···π stacking interactions are highlighted as yellow dashed circles.

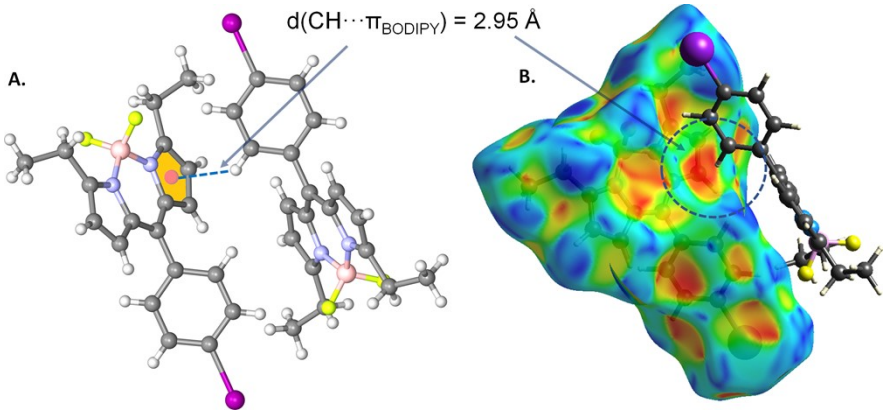

Figure S30 A) The CH···π_{BODIPY} interaction in **B3**. B) and C) Hirshfeld surfaces of **B3** mapped with shape index, showing areas of CH···π stacking interactions highlighted as black dashed circles.

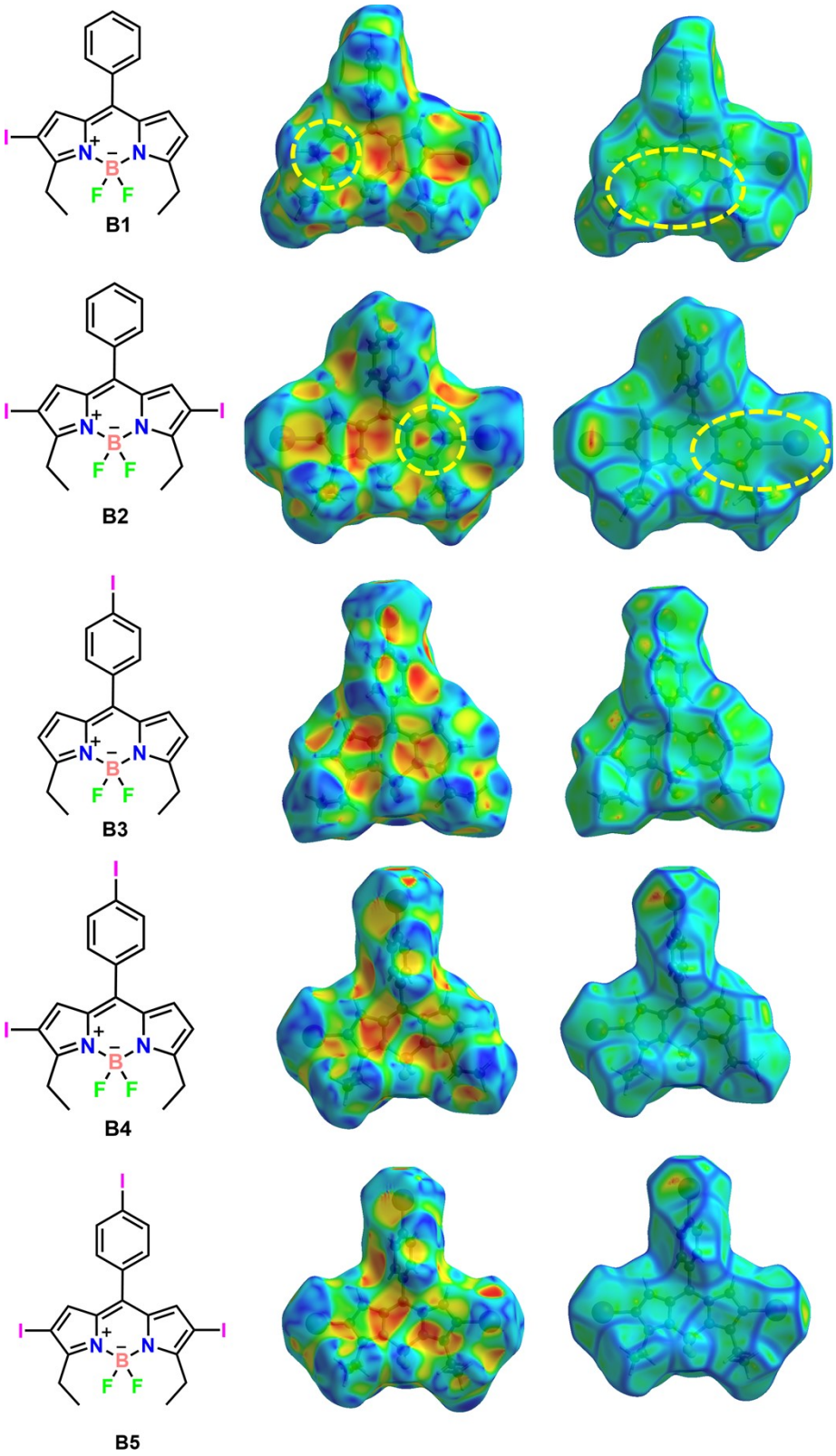

Fig. S31 Perspective views of Hirshfeld surfaces mapped with shape index (second column) and curvedness (third column) of compounds B1-B5.

REFERENCES

1 E. T. Eçik, E. Şenkuytu, Z. Cebesoy and G. Y. Çiftçi, *RSC Adv.*, 2016, **6**, 47600–47606.

2 W. Wu, H. Guo, W. Wu, S. Ji and J. Zhao, *J. Org. Chem.*, 2011, **76**, 7056–7064.

3 M. A. Spackman and D. Jayatilaka, *CrystEngComm*, 2009, **11**, 19–32.

4 M. A. Spackman and J. J. McKinnon, *CrystEngComm*, 2002, **4**, 378–392.

5 M. J. Turner, J. J. McKinnon, S. K. Wolff, D. J. Grimwood, P. R. Spackman, D. Jayatilaka and M. A. Spackman, 2017.

6 J. J. McKinnon, D. Jayatilaka and M. A. Spackman, *Chem. Commun.*, 2007, 3814–3816.

7 J. J. McKinnon, M. A. Spackman and A. S. Mitchell, *Novel tools for visualizing and exploring intermolecular interactions in molecular crystals*, 2004, vol. 60.